Noble gas magmatic signature of the Andean Northern Volcanic Zone from fluid inclusions in minerals

J. Lages [a,*], A.L. Rizzo [b], A. Aiuppa [a,b], P. Samaniego [c], J.L. Le Pennec [c], J.A. Ceballos [e], P.A. Narváez [f], Y. Moussallam [c,d], P. Bani [c], C. Ian Schipper [g], S. Hidalgo [h], V. Gaglio [a], E. Alberti [a] and A. Sandoval-Velasquez [a]

Author's affiliations:

[a] Dipartimento DiSTeM, Università degli Studi di Palermo, Palermo, Italy

[b] Istituto Nazionale di Geofisica e Vulcanologia, Sezione di Palermo, Palermo, Italy

[c] Université Clermont Auvergne, CNRS, IRD, OPGC, Laboratoire Magmas et Volcans, Clermont-Ferrand, France

[d] Lamont-Doherty Earth Observatory, Columbia University, New York, USA

[e] Servicio Geológico Colombiano - Observatório Vulcanológico y Sismológico de Manizales, Colombia

[f] Servicio Geológico Colombiano, Observatório Vulcanológico y Sismológico de Pasto, Colombia

[g] School of Geography, Environment and Earth Sciences, Victoria University of Wellington, Wellington, New Zealand

[h] Instituto Geofísico - Escuela Politécnica Nacional, Quito, Ecuador

*** Corresponding author:** Joao Lages; joaopedro.nogueiralages@unipa.it

Abstract

Trace volatile elements like He are key for understanding the mantle source signature of magmas and to better constrain the relative roles of subduction and crustal processes to the variability of along-arc chemical and isotopic signatures of magmatic fluids. Here we report on noble gas abundances and isotopic data of Fluid Inclusions (FIs) in eruptive products and/or fumarolic gases from the Colombia-Ecuador segment of Andean Northern Volcanic Zone (NVZ). FIs in olivine phenocrysts from Ecuador (El Reventador, Cotopaxi and Tungurahua) yield air-normalized corrected $^3He/^4He$ ratios of 7.0-7.4 R_A, within the MORB range (8±1 R_A). With exception of the Cotopaxi lavas (opx<<Oliv.), these are indistinguishable of those obtained for their cogenetic orthopyroxene pairs and of gas emissions previously reported in literature. Olivine phenocrysts from Nevado del Ruiz fissure lavas also yield the highest $^3He/^4He$ (8.5±0.3 R_A) for this volcanic system, which is in the range of fumarolic gases for Galeras (previously reported as high as 8.8 R_A and here measured to a maximum of 8.3±0.1 R_A). Our dataset highlights disparities between isotope signatures of eruptive products from Ecuador (avg. ~7.2 R_A) and those reported for the Colombian portion of the NVZ (avg. ~8.5 R_A). Previous studies on the geochemistry of erupted products put in evidence significant along-arc variations ascribed either to the involvement of different slab components, or to variable depths of evolution of arc magmas within the continental crust. However, the same variation is not discernible in the signature of noble gases, especially helium, from FIs and gas emissions analyzed in this study, with little inter-variation between Cotopaxi, Reventador and Tungurahua (all within 0.2 R_A from the Ecuador average of 7.2) and Galeras and Nevado del Ruiz, whose maximum values differ by ~0.3 R_A. We therefore suggest a homogenous MORB-like $^3He/^4He$ signature for the mantle wedge beneath this arc segment, whereby along-arc variations in crustal thickness (from <35 km at the northernmost part of the segment to ≥50 km at the Ecuadorian arc segment) may factor largely into the variability recorded on our data set. The first $CO_2/^3He$ ratios obtained in FIs from Andean rocks support the hypothesis of increasing crustal contamination from Colombia to Ecuador, concomitant with increasing crustal thicknesses under the respective arc regions.

Keywords *Andean Volcanic Belt; Northern Volcanic Zone; fluid inclusions; noble gases; helium; crustal thickness;*

1. Introduction

Due to their inert behavior and large isotope ratio variability among the different Earth's reservoirs, noble gases such as He, Ne and Ar are considered optimal tracers to constrain mantle geochemical features and the key processes that contribute to modifying deep magmatic sources (e.g., Gautheron and Moreira, 2002; Martelli et al., 2014; Rizzo et al., 2018). In addition, noble gases may help in evaluating the complex migration processes of magmatic fluids from the Earth's mantle to the atmosphere, hydrosphere and crust (e.g., Porcelli and Wasserburg, 1995a; Farley and Neroda, 1998; Ozima and Igarashi, 2000; Porcelli et al., 2001; van Keken et al., 2002; Ballentine et al., 2002; Moreira, 2013; Rizzo et al., 2015; Boudoire et al., 2018). These volatiles can be primordial in origin, trapped in the mantle since planetary accretion, produced in-situ, or they may be recycled into the mantle via material originally at the surface through subduction (e.g., Jackson et al., 2013; Kobayashi et al., 2017; Smye et al., 2017). Seismic tomography studies point out that oceanic plates can be subducted well below the 670 km discontinuity down to the core-mantle boundary (e.g., van der Hilst et al., 1997; Bijwaard and Spakman, 1998; Fukao et al., 2001). Additionally, numerical modelling of mantle convection patterns (van Keken and Ballentine, 1999) casts doubt upon the likelihood of maintaining a deep region of the mantle isolated over geological timescales. Noble gas chemistry of magmatic fluids in volcanic arcs shows $^3He/^4He$ isotope variations ranging from 10.1 to 0.01 R_A (Hilton et al., 2002; Sano and Fischer, 2013). While $^3He/^4He$ ratios > 9.5 R_A (reported for example by Jean-Baptiste et al., 2016 for the Vanuatu arc) have been attributed to the contribution of the incipient plume at the westernmost edge of the Pacific super-plume (Montelli et al., 2006), $^3He/^4He$ ratios lower than Mid-Ocean Ridge Basalt (MORB, 8±1 R_A, Graham, 2002; Graham et al., 2014) have been interpreted as a result of either (i) the subducted slab component, including altered oceanic crust and oceanic sediments (Di Piazza et al., 2015; Robidoux et al., 2017; Battaglia et al., 2018); (ii) shallow-derived He resulting from interactions between the rising magma and the continental crust overlying the volcanic arc (Sano and Wakita, 1985a; Sano and Fischer, 2013); and/or (iii) the influence and nature of continental crust subducted beneath volcanic arcs (e.g., Southern Italy; Hilton et al., 2002; Martelli et al., 2014 and references therein).

To better determine the relative contributions of subduction-related parameters (e.g., convergence rate, slab dip, slab age, etc.) and crustal processes (crustal thickness and magma-residence time in the crust) to the observed along-arc $^3He/^4He$ variations, it is crucial to account for the space-time variability of available data so far reported in the literature for arc volcanism. Geographic controls on $^3He/^4He$ signatures have been assigned to either magma aging or interaction with surrounding country rock (e.g. Marty et al., 1989; Hilton et al., 1993a; Van Soest et al., 1998; Notsu et al., 2001; Hilton et al., 2002), especially in far-from-vent areas where degassing occurs less vigorously. Both processes can add a radiogenic helium component to mantle-derived melts and therefore decrease $^3He/^4He$ ratios (<<MORB), such as those observed in hydrothermal fluids. Also, it must be considered that the use of standard sampling techniques for noble gas extraction from high-temperature fumaroles (Sano et al., 1990; Giggenbach et al., 1993 and references therein) requires direct access to outpouring vents often located at hazardous volcanic areas. In other cases, surface manifestations of volcanic degassing are absent from quiescent stages of activity. Such scenarios make noble gas volcanic gas-based characterization of volcanic centers more difficult.

In addition to the spatial $^3He/^4He$ variability around individual volcanoes, temporal He isotope changes have been commonly reported in many active volcanoes (Sano and Fischer, 2013). Several studies exist of temporal fluctuations of $^3He/^4He$ ratios, correlating well with changes in volcanic activity. These include Mt. Etna (Caracausi et al., 2003; Rizzo et al., 2006; Paonita et al., 2012, 2016) and Stromboli, in Italy (Capasso et al., 2005; Rizzo et al., 2009, 2015a), at Mount Ontake, in Japan (Sano et al., 2015), Santorini, in Greece (Rizzo et al., 2015b), and at Turrialba, in Costa Rica (Rizzo et al., 2016). Such phenomena attest to the fact that He isotope signatures measured at the surface might be affected by processes happening deep in the magma chamber, including the input of new magma as volcanic activity escalates.

Because of spatial/temporal variability, and due to the fact that some arc volcanoes remain unsampled to date, mostly due to their remoteness and inaccessibility, arc-scale noble gas compositional catalogues (Hilton et al., 2002; Sano and Fischer, 2013) remain biased by the incomplete and heterogeneous data set available. Nonetheless, global reviews (Hilton et al. (2002), Sano and Fischer (2013), Oppenheimer et al. (2014) and Mason et al. (2017) provide convincing evidence for arc-scale correlations between isotope tracers and slab/crustal processes.

Despite the high density and intense activity of NVZ volcanoes, few studies exist up to date dealing with their noble gas isotope signature (Hilton et al., 2002). High temperature (>300˚C) fumarole data have only been reported for Galeras (Sano and Williams, 1996; Sano et al., 1997). These provide an opportunity to sample volatiles released directly from magma at depth. Lower temperature emissions (e.g., bubbling hot springs), located on the flanks of volcanoes. allow for the sampling of noble gases released through hydrothermal systems. The overall dominance of low temperature noble gas data for NVZ volcanoes led Hilton et al. (2002) to estimate $^3He/^4He$ averages for Colombia and Ecuador of 5.66± 2.41 and 3.22± 0.98, respectively. These are far below the expected MORB range (8± 1). This study focus on improving the current dataset for the Northern Volcanic Zone, by reporting on new noble gas data from fluid inclusion analysis in olivine and pyroxene phenocrysts from five of the most active volcanoes in the entire Andean Volcanic Arc, Tungurahua, El Reventador and Cotopaxi in Ecuador, and Galeras and Nevado del Ruiz in Colombia. These data are integrated with the first measurements of CO_2 concentration ($CO_2/^3He$ ratios) in fluid inclusions (FIs) from Andean rocks to further constrain the geochemical features of the magmatic source underlying these volcanic centers. Finally, our investigation provides new information on the processes governing the variations in noble gas compositions along the Northern Volcanic Zone.

2. Geodynamic and geological setting

The Andes are a continental volcanic arc formed by the subduction of the 12-20 Ma old Nazca plate slab (Jarrard, 1986) beneath the South American plate, occurring at a rate of about 50-70 mm/yr (Trenkamp et al., 2002; Nocquet et al., 2014). This volcanic chain extends for over 7000 km along the western margin of South America and volcanism there occurs in four separate regions: the Northern (NVZ), Central (CVZ), and Southern (SVZ) volcanic zones, as a result of the subduction of the Nazca plate; and the Austral (AVZ) volcanic zone originating on the convergent plate boundary between the Antarctic plate and the continental South American plate (Fig. 1A). The Colombian segment of the NVZ is defined by a narrow volcanic arc (Fig. 1B) located above the Benioff zone that clearly defines a steep subduction slab (Ojeda and Havskov, 2001) exhibiting lateral variations in the dip angle, from ~20°-35° north of the Carnegie Ridge (Pennington, 1981) to ~25° beneath Ecuador (Guillier et al., 2001; Kendrick et al., 2003; Yepes et al., 2016; Fig. 1C). This change in dip angle underneath Ecuador causes the volcanic arc to widen and split into three segments, the frontal arc (Western cordillera), the main arc (Eastern Cordillera) and the back-arc dominated by dacitic, andesitic and shoshonitic products, respectively (Hall et al., 2008; Hall and Mothes, 2008; Hidalgo et al, 2012; Ancellin et al, 2017). The documented along-arc variations in subduction parameters (e.g., Syracuse et al., 2010) and in the chemical/isotopic signature of the eruptive volcanites (e.g., Ancellin et al. 2017) make the Andes, and in particular the NVZ, a unique geodynamic setting to test for the influence of varying subduction geometries and thermal regimes on the noble gas fluid signature along the arc.

3. Petrological and eruptive background

In volcanic arc segments such as the Ecuador-Colombia magmas inherit their compositional signatures from multiple sources, including: (i) the dehydration/partial melting of the subducting sediments/oceanic crust; (ii) the mantle wedge; and (iii) the overlying continental crust (Hickey et al., 1986; Hildreth and Moorbath, 1988; Tatsumi, 1989; Stern 2002). Andean magmas range considerably in composition and the prevailing andesites attest for the severe processing of primary melts along the arc. In fact, experiments (Nicholls and Ringwood, 1972; Mysen et al., 1974) and analysis of natural samples (Reubi and Blundy, 2009) both show that andesites mainly form as the product of differentiation processes such as fractional crystallization, coupled with crustal assimilation and magma mixing (Grove et al., 2003; Kelemen et al., 2014; Schmidt and Jagoutz, 2017). On the other hand, recent studies highlight the fact that primitive arc magmas are intrinsically heterogeneous (Turner et al., 2016; Schmidt and Jagoutz, 2017), an important member of this family being the so-called magnesian andesites that are considered as direct by-products of mantle melting (e.g., Grove et al., 2003) and that are regularly found along the Ecuadorian volcanic arc (e.g. Samaniego et al., 2010). These processes not only impart chemical and textural signatures on the resulting eruptive products (Panter et al., 1997; Schiano et al., 2010; Garrison et al., 2011; Lee and Bachmann, 2014), but can also alter to various degrees the isotope signature of deep magmatic fluids.

3.1 The colombian arc segment (CAS)

3.1.1 Nevado del Ruiz

The Nevado del Ruiz Volcanic Complex (CVNR) is located in the department of Caldas, near the northern end of the NVZ. Its history can be subdivided into four main eruptive phases, culminating in the Second Ruiz Eruptive Stage that included effusive-to explosive activity (Thouret et al., 1990). Over the past 11 ka, the volcano has erupted andesitic to dacitic magmas (about 40% dacites and 60% andesites; Vatin-Pérignon et al., 1990). Despite the complex eruptive history of Nevado del Ruiz, its geochemical evolution suggests a common magmatic source over time (see Vatin-Pérignon et al., 1990). In this study, we focused on the fissure lavas of *La Esperanza*, located in the northernmost sector of the volcanic complex. This segment is believed to be structurally controlled by the *Villamaría–Termales* fault system, which possibly provided the linear fractures through which these lavas were erupted (Martinez et al., 2014). Due to its stratigraphic position and moderate glacial processing, the age of this unit has been estimated at ~0,035 – 0,045 Ma. The presence of olivine microphenocrysts within microcrystalline-microlytic to moderately intergranular textures, clearly distinguishes these lavas from the majority of the eruptive periods of the volcanic complex that exhibit lower fractions of mafic minerals (25-45% overall in CVNR products; Vatin-Pérignon et al., 1990; Martínez et al., 2014).

3.1.2 Galeras

The Galeras Volcanic Complex (GVC) is located approximately 60 km north of the Colombia-Ecuador border. Over the past 1 Ma it has been characterized by caldera-forming eruptions, followed by the construction of new active cones that produced lavas and pyroclastic flows, ranging from basaltic-andesites to dacites (Calvache and Williams, 1997a and b). Its Holocene active cone lies on the eastern side of the volcanic complex and produced the basaltic-andesite products analyzed in this study. These were interpreted as possible fissure lavas (Calvache, 1990) that extend for an average length of 1.8 km and are located ~3-4 km away from the Galeras central crater. Plagioclase and pyroxene are the main mineral phases in these lavas, but fresh olivine is common (Calvache, 1990). Considering the location of the lava flow outcrops, Calvache (1990) argued that these lavas may have erupted with a high effusion rate in order to travel such long distances. Their well-preserved morphology suggests an approximate age between the pyroclastic flow deposits of 1100 y BP and the major eruption of 1866 CE (Calvache, 1990).

3.2 The ecuadorian arc segment (EAS)

3.2.1 El Reventador

Although geographically located in the Ecuadorian back-arc, El Reventador displays a typical Main Arc geochemistry. A large sector collapse around 19,000 y BP left a prominent 4 km-wide volcanic collapse scar (Aguilera et al., 1988). Since then, a young, symmetrical, 1 km-high volcanic cone has grown to be one of the most active volcanoes in the Ecuadorian Andes. After 26 years of quiescence, the volcano initiated a new period of intense volcanic activity starting with a sub-Plinian event in November 3, 2002, rapidly followed by two lava flows effusively emplaced over a two-month period after the reactivation of the system (Samaniego et al., 2008). Petrological analysis of products from the 2002 eruption suggests that there was a single pre-eruptive reservoir with a top at 8 ± 2 km and a base at 11 ± 2 km (Ridolfi et al., 2008;

Samaniego et al., 2008). The same authors reported on the geochemical and mineralogical characteristics of the 2002 and later-emplaced 2004-2005 lava flows with overall silica contents ranging 56-59 wt.%. In this study we analyzed the 2009 lava flows consisting of medium-high K basaltic andesites to andesites, that display similar compositions to those reported for the initial 2002 eruptive products (porphyritic, ~25 – 30 vol.% phenocrysts in pyroclastic blocks and ~40 vol.% in lava flows), with a mineral assemblage composed of plagioclase, clinopyroxene, orthopyroxene, amphibole, magnetite, with scarce olivine (Samaniego et al., 2008).

3.3.2 Cotopaxi

Cotopaxi, a stratovolcano located ~60 km south of Quito, on the Main Arc, has exhibited a history of bimodal volcanism, where rhyolitic and andesitic magmas erupt in quick succession, apparently from the same vent, displaying very limited intermingling (Hall and Mothes, 2008). Each eruption cycle has been characterized by a similar eruptive pattern, involving plinian scoria or pumice tephra falls, scoria or pumice pyroclastic flows, blocky-lava flows, and widespread debris flows. From the end of the Colorado Canyon episode 4,000 years ago until the present, Cotopaxi has experienced a continuous series of periodic eruptions, all of which have involved andesitic magmas, with 57–62% SiO_2 (Hall and Mothes, 2008, Pistolesi et al., 2011) and phenocryst assemblages that include plagioclase, orthopyroxene, clinopyroxene, magnetite, and rare olivine. The younger products of Cotopaxi IIB comprise a series of andesitic scoria falls, lava flows and a single rhyolite eruption. In the lavas from Cotopaxi IIB olivine is occasionally present in trace amounts, but increases up to 2% (Hall and Mothes, 2008) in the youngest rocks analyzed in this study.

3.3.3 Tungurahua

Tungurahua is a stratovolcano located in central Ecuador on the Main Arc. Historical records (Martinez, 1932) and chronological data of the eruptive products of Tungurahua (Hall et al., 1999; Le Pennec et al., 2008) reveal that regional tephra fallouts, blocky lava flows, pyroclastic flows and related debris flows (such as the 1100 y BP analyzed in this study), characterized most eruptions in recent times. A recurrence rate of at least one pyroclastic flow-forming eruption per century was established for the last millennium, ranking Tungurahua amongst the most active volcanoes of the Northern Andes (Le Pennec et al., 2008). More recent eruptive products, such as pyroclastic flows, tephra deposits and lavas display andesitic compositions (58–59 wt% SiO_2; Samaniego et al., 2011) and contain plagioclase (5–15 vol.%), clinopyroxene (2–4 vol.%), orthopyroxene (2–4 vol.%), and magnetite, with trace olivine. This is similar to compositions reported by Samaniego et al. (2011) for the 2006 juvenile blocks from the pyroclastic flow deposits also analyzed in this study, which are dark, vesicular, porphyritic (~10–20 vol.% phenocrysts) andesites (57.6–58.9 wt.% SiO_2) composed of similar mineral assemblage.

4. Methods and analysis

4.1 Noble gases in Fluid Inclusions

Although our study does not offer petrographic evidence of FI in olivine and pyroxene phenocrysts, it is generally assumed that these phases often contain primary and secondary FI that are trapped during crystal growth in the magma. The element and isotope compositions of He, Ne, and Ar in olivine- and orthopyroxene-hosted fluid inclusions (FIs) were measured at the noble gas laboratory facilities at the *Istituto Nazionale di Geofisica e Vulcanologia* (*INGV*) in Palermo. Phenocrysts (0.25 to 0.50 mm fractions) were separated from lavas and scoriae layers from Nevado del Ruiz, Galeras, El Reventador, Cotopaxi and Tungurahua using sodium polytungstate (SPT) heavy liquid. The individual crystals without impurities were then carefully handpicked under a binocular microscope and cleaned in multi-stage ultra-sonic baths (e.g., Di Piazza et al., 2015; Rizzo et al., 2015, 2018). For analysis, the samples were accurately weighed and loaded into a stainless-steel crusher for noble gas extraction. The gases were consequently released by in-vacuo single-step crushing of minerals at about 200 bar applied by a hydraulic press, which minimizes the contribution of in-situproduced He, such as cosmogenic ^{3}He and radiogenic ^{4}He possibly trapped in the crystal lattices (e.g., Scarsi, 2000). The Total Gas Content (TGC) was first quantified during noble-gas extraction at the time of crushing by measuring the total gas pressure (CO_2+N_2+O_2+noble gases) and subtracting the residual pressure oses after removing CO_2 using a "cold finger" immersed in liquid N_2 at –196°C. Residual gases were then cleaned under getters in an ultra-high-vacuum (10^{-9}–10^{-10} mbar) purification line, and all species in the gas mixture, except noble gases, were removed. A "cold finger" with active charcoal immersed in liquid N_2 then removed Ar, while He and Ne were separated by using a cold head cooled at 10K and then moved at 40 and 80K in order to release He and Ne, respectively.

Helium (^{3}He and ^{4}He) and Ne (^{20}Ne, ^{21}Ne, and ^{22}Ne) isotopes were measured separately by two different split-flight-tube mass spectrometers (Helix SFT-Thermo). The $^{3}He/^{4}He$ ratios are expressed in units of R/R_A (where R_A is the $^{3}He/^{4}He$ of air; 1.39×10^{-6}). The analytical uncertainty of He-isotope ratio measurements (1σ) was <4% (except for the pyroxene phenocrysts from Cotopaxi whose uncertainty was 13.5%), whereas in Ne-isotope ratios (1σ) was <1.7% and <4.6% for $^{20}Ne/^{22}Ne$ and $^{21}Ne/^{22}Ne$, respectively. The reported values of both Ne-isotope ratios are corrected for isobaric interferences at m/z values of 20 ($^{40}Ar^{2+}$) and 22 ($^{44}CO_2^{2+}$; Rizzo et al., 2018). Argon isotopes (^{36}Ar, ^{38}Ar, and ^{40}Ar) were analyzed by a multicollector mass spectrometer (GVI Argus) at an analytical uncertainty of $^{40}Ar/^{36}Ar$ <0.5%. A pre-purified air standard subdivided in tanks was used for He, Ne, and Ar elemental and isotopic recalculations. The analytical reproducibility of ^{4}He, $^{3}He/^{4}He$, $^{20}Ne/^{22}Ne$, $^{21}Ne/^{22}Ne$, and ^{40}Ar of standards were <2.4%, <2.6%, <0.4%, <0.5%, and <2.4%, respectively. These values represent the standard deviation of measurements made during >1 year of analyses for He and Ne and ~4 years for Ar, in the same source setting conditions. Typical blanks for He, Ne, and Ar were $<10^{-15}$, $<10^{-16}$ and $<10^{-14}$ mol, respectively. Further details on sample preparation and analytical procedures are available in Di Piazza et al. (2015) and Rizzo et al. (2015, 2018).

4.2 Dry fumarolic gas sampling and Noble gas isotope analysis

Dry gas samples for the analyses of He, Ne, and Ar were collected in the flanks of the active central crater of Galeras on 14 July 2017. Fumarolic gas from two steaming vents (at temperatures of 91.3 and 87.5°C) was collected in two-way Pyrex bottles with vacuum valves at both ends. Despite the apparent weak flux and in-situ low temperatures measurements (close to boiling), the gas was channeled through a stainless-steel tube and propelled several times through the sampling circuit in order to eliminate any possible remains of atmospheric components within the sampling lines.

The concentration and isotope compositions of He, Ne and Ar in fumaroles were measured by admitting the gases into three distinct ultra-high-vacuum (10^{-9}–10^{-10} mbar) purification lines, in which all of the species in the gas mixture, except noble gases, were removed. Prior to the analysis, He and Ne were separated from Ar by adsorbing the latter in a charcoal trap cooled by liquid nitrogen (77 K). He and Ne were then adsorbed in a cryogenic trap connected to a cold head cooled with a He compressor to ≤10 K. He was desorbed at 42 K and admitted into a GVI-Helix SFT mass spectrometer. After restoring the ultra-high vacuum in the cryogenic trap, Ne was released at 82 K and then admitted into a Thermo-Helix MC Plus mass spectrometer. Ar was purified only under getters and finally admitted in a GVI-Helix MC. The analytical uncertainty of He-isotope ratio measurements (1σ) was <0.9%, while that of Ne- and Ar-isotope ratio was <0.1%. The same procedure was adopted for the He, Ne and Ar isotope measurements of the air standards (e.g., Rizzo et al., 2016), whose reproducibility conditions are comparable to those reported for FIs (see Section 4.1). Typical blanks for He, Ne, and Ar were $<10^{-15}$, $<10^{-16}$ and $<10^{-14}$ mol, respectively. Helium isotope ratios are reported in the form of R_C/R_A, where R_C is the air-corrected $^3He/^4He$ ratio of the sample, assessed based on $^4He/^{20}Ne$ ratios:

$$R_C/R_A = [(R_M/R_A)(He/Ne)_M - (He/Ne)_{air}]/[(He/Ne)_M - (He/Ne)_{air}]$$

where subscripts "M" and "air" refer to measured and atmospheric theoretical values, respectively. Across our dataset, R_C/R_A ratios are on average 2% higher than those uncorrected and 3 analysis required corrections outside of quoted R_C/R_A errors (Tab. 1). Argon isotope ratios account for atmospheric-corrected ^{40}Ar, assuming that all ^{36}Ar contained in the gas phase is of atmospheric origin:

$$^{40}Ar^* = {}^{40}Ar_m - [({}^{40}Ar/{}^{36}Ar)_{air} \times {}^{36}Ar_m],$$

where $^{40}Ar^*$ represents the corrected isotope value and m indicates the measured value (Marty and Ozima, 1986 and references therein). These differ by as much as two orders of magnitude in opx phenocrysts from Cotopaxi (see Tab. 1).

5. Elemental and isotopic compositions of He, Ne, Ar and CO_2

5.1 Fluid inclusions in olivine and orthopyroxene phenocrysts phases

Noble gas abundances and isotope results obtained from single-step crushing olivine and orthopyroxene phenocrysts phases from scoriae layers and lava flows from Colombia (Galeras and Nevado del Ruiz) and Ecuador (Cotopaxi, El Reventador and Tungurahua) are listed in table 1. These yield R_C/R_A values as high as 8.5 R_A (measured in olivine from Nevado del Ruiz), and as low as 2.2 R_A (obtained in FIs trapped within orthopyroxene phenocrysts from Cotopaxi; Fig. 2). With exception of the former, all $^3He/^4He$ isotope values fall within the typical range found in arc-related FIs and free gases globally (Hilton et al., 2002; Sano and Fischer, 2013; Mason et al., 2017). Helium abundances range from 0.12 - 3.23 $\times10^{-13}$ mol g^{-1} in orthopyroxene and 1.68 - 17.7 $\times10^{-13}$ mol g^{-1} in olivine (Fig. 3A). Despite the contrast in gas contents, mineral pairs show indistinguishable R_C/R_A ratios (Tab. 1), the exception being the two mineral pairs from Cotopaxi lavas which also yield distinct $^3He/^4He$ ratios (opx<oliv.; Fig. 3B). Olivine phenocrysts from Galeras and Nevado del Ruiz lavas yield He concentrations between 0.24 and 1.19 ($\times10^{-13}$ mol g^{-1}). $^{40}Ar/^{36}Ar$ isotope ratios range from 297.9 to 471.7 (avg. of 328.3 across all samples), supporting a prevalent atmospheric derivation ($^{40}Ar/^{36}Ar$ in air = 295.5) and confirming the $^{40}Ar/^{36}Ar$ ratio range observed in the fumarolic gases from Galeras central crater (297.0 and 302.1; Fig. 2).

Our results imply Ar isotope ratios well below those characteristic of the upper mantle ($^{40}Ar/^{36}Ar \sim 40{,}000$; Fischer et al., 2005). Nonetheless, these fall within the typical range of subduction-related volcanism (Hilton et al., 2002; Sano and Fischer, 2013), even in opx from Ecuadorian samples which consistently show lower $^{40}Ar/^{36}Ar$ than those of cogenetic olivine. Atmospheric contamination is also reflected in the $^4He/^{20}Ne$ ratios here reported, that vary from 2.2 in orthopyroxenes from Cotopaxi (also the lowest $^3He/^4He$ obtained analytically) to 522.3 measured in Olivine phenocrysts from El Reventador (Fig. 2; atmospheric $^4He/^{20}Ne$ = 0.318; mantle air-free gases are generally characterized by values ≥ 1000; e.g., Rizzo et al., 2018). Olivine phenocrysts also yield systematically higher $^4He/^{20}Ne$ ratios than their cogenetic orthopyroxene pairs (Tab. 1).

Concentrations of CO_2 obtained in olivine fluid inclusions from Nevado del Ruiz (0.16×10^{-9} mol g^{-1}) and Galeras (0.62 and 0.31×10^{-9} mol g^{-1}) were in the range of CO_2 contents measured in orthopyroxene phenocrysts from Ecuadorian volcanoes (only as high as 8.63×10^{-9} mol g^{-1} in opx from Reventador) and considerably lower than CO_2 concentrations measured across their olivine separates (up to 69.4×10^{-9} mol g^{-1} in Reventador samples; Tab. 1). Estimated $CO_2/^3He$ ratios span from 6.13 (in olivines from Reventador) to 0.28×10^9 (measured in orthopyroxene phenocrysts from Tungurahua; Tab. 1). The carbon isotope characterization of NVZ fluids was not possible due to the gas-poor nature of the inclusions, in which carbon was not sufficiently abundant to allow further analysis after the noble gases had been extracted.

5.2. Isotope geochemistry of fumarolic gases

Sampling details and analytical data from fumarolic discharges measured at the central crater of Galeras are provided in table 2. The high R_C/R_A values (8.3 and 8.2 R_A, and $^4He/^{20}Ne$ of 7.3 and 29.6, respectively) are in agreement with values reported by Sano and Williams (1996) and Sano et al. (1997) for nearby fumarolic discharges (Fig. 2). Argon isotope values also show very limited variability between the two near sites, with $^{40}Ar/^{36}Ar$ of 297.9 ± 0.1 and 302.1 ± 0.2, respectively. Figure 2 shows the new isotope geochemistry data from fumarolic gases and FIs integrated with existing literature data for all 5 volcanoes studied (Ecuador and Colombia).

6. Discussion

In order to assess local and regional isotope variations along the Northern Volcanic Zone it is crucial to account for the various processes that have the potential to mask the geochemical characteristics of the deep mantle source underlying the northernmost segment of the Andean Volcanic Arc. In volcanic gases, close-to-MORB or within-MORB $^3He/^4He$ ratios are commonly measured along volcanic front regions where direct input of magma occurs (e.g. Sano and Wakita 1987; Sano and Wakita 1988a; Giggenbach et al., 1993; Hulston et al., 2001; Umeda et al., 2007; Di Piazza et al., 2015; Robidoux et al., 2017; Battaglia et al., 2018; Rizzo et al., 2019). Tectonically active regions such as the Andes provide a wide range of sampling media for noble gases, especially through active volcanism (Hilton et al., 2002; Aguilera et al., 2012; Benavente et al., 2016; Lopez et al., 2018). Surface discharges of magma degassing at depth can vary largely in nature and are typically found in the vicinity of active craters (as high-temperature fumarolic gas), and/or in peripheral areas as geothermal fields and low-temperature bubbling springs. Such variability had some studies reporting a wide range of $^3He/^4He$ isotope signatures within individual volcanic systems, such as Sano et al. (1984), following their study of Mt. Ontake in Japan, and Williams and Sano (1987) at Nevado del Ruiz, in Colombia. These studies typically reveal decreasing $^3He/^4He$ ratios with increasing distance from volcanic craters, indicating that despite effectively carrying magmatic volatiles to the atmosphere, volcanic steam escaping through fractures/soil around peripheral areas is increasingly contaminated by crustal fluids (in comparison to high-temperature, summit discharges).

On the other hand, primary noble gas compositions in fluid inclusions may be affected by post-eruption ^4He in-growth and diffusion-controlled isotope fractionation. These processes are discussed in detail in supplementary material S1. However, predominantly MORB-like $^3He/^4He$ isotope ratios obtained in this study suggest that diffusive fractionation plays a minor role in our dataset. Differences in the chemistry of FIs obtained in orthopyroxene and olivine, in part expected due to the lower effective closure temperature and pressure of pyroxenes (that continue to exchange helium with the magma after olivine had been closed), are also not observed systematically (Fig. 3; see also supplementary material S1).

6.1. Atmospheric contamination

Due to their high concentration in the atmosphere, light noble gases such as Ar are more susceptible to atmospheric contamination. In subduction-related volcanism, Ar-isotope ratios are systematically low and close to theoretical values in the atmosphere (Hilton et al., 2002; Martelli et al., 2014; Di Piazza et al., 2015; Rizzo et al., 2015, 2016, 2019; Robidoux et al., 2017; Battaglia et al., 2018). This is even more pronounced when compared to those from intra-plate or ridge environments (e.g., Burnard et al., 1997; Moreira et al., 1998; Ballentine et al., 2005; Boudoire et al., 2018; Rizzo et al., 2018). Figure 2A confronts our new results to those reported in the literature for high- and low-temperature free gases and shows that variable extents of air contamination affected nearly all the $^{3}He/^{4}He$ ratios reported. Similarly, $^{40}Ar/^{36}Ar$ values (Fig. 2B) are well below the theoretical MORB-like mantle ratio ($^{40}Ar/^{36}Ar$ ~30,000 to 40,000; Burnard et al., 1997; Moreira et al., 1998) or typical mantle-derived samples (e.g., Kaneoka, 1983; Ozima and Podosek, 1983; Allègre et al., 1987; Rizzo et al., 2018). As many authors have suggested over the years (e.g., Gurenko et al., 2006; Di Piazza et al., 2015; Rizzo et al., 2018)), the trend observed may indicate mantle contamination at depth from atmospheric Ar derived from dehydration of the subducting oceanic crust.However, a minimum contribution associated with crystals exposure to the atmosphere cannot be ruled out (see also supplementary material S2 for atmospheric components in the Neon isotope systematics)

6.2. Inferences on local and regional $^{3}He/^{4}He$ isotope signatures

The overprint of noble gas mantle signatures, especially helium, has always appeared quite significant in the northernmost region of the Andean Volcanic Arc. Negative correlations between $^{3}He/^{4}He$ and distance from active volcanic craters are common (Sano et al.,1984; Williams and Sano, 1987; Sano and Wakita 1992; Sano, et al., 1994; van Soest et al., 1998; Sano and Nakajima, 2008), as degassing of fresh, uncontaminated magma supplies helium that disperses through continental lithologies in which radiogenic ^{4}He is abundant (see Sano et al., 1990 and Sano et al., 2012 for details on hydrodynamic dispersion models of helium at active volcanic systems such as Nevado del Ruiz). Previous global compilations of helium isotope data (e.g. Hilton et al., 2002; Sano and Fischer, 2013; Oppenheimer et al., 2014; Mason et al., 2017) reported $^{3}He/^{4}He$ averages of 3.2 ± 1.0 R_A and 5.7 ± 2.4 R_A (<< MORB-range of 8 ± 1 R_A) for Ecuador and Colombia, respectively (e.g., Hilton et al., 2002). These may in large reflect significant extents of mixing between mantle-derived and radiogenic helium produced in the crust. For instance, an extensive study by Inguaggiato et al. (2010) that reported on the geochemical signature of 56 thermal and cold waters sites, as well as 32 dissolved gases and 27 bubbling springs, collected north-south along the Ecuadorian arc, obtained a wide range of helium isotope results, from 0.1 and 7.1 R_A.

As a result, deep mantle noble gas isotope signatures can be overprinted, especially in regions characterized by older, flatter dipping slabs such as in the south of Ecuador (Barazangi and Isacks, 1979; Gutscher et al., 1999). Actively degassing volcanoes, especially those with accessible high-temperature fumarolic fields such as Galeras, Cumbal, Cerro Machin and Purace, were successfully sampled in the past (Sano and Williams, 1987; Sano et al., 1990; Sturchio et al., 1993; Sano and Williams, 1996; Sano et al., 1997; Lewicki et al., 2000), with maximum $^{3}He/^{4}He$ isotope ratios reported of 8.8, 7.9, 6.8 and 7.1 R_A, respectively. However, for large portions of the arc, helium isotope signatures remained uncharacterized.

Here we provided the first helium isotope constrains on the mantle sources feeding the volcanic systems of Cotopaxi, Tungurahua and El Reventador, for which only peripheral gas data were reported in the past (Inguaggiato et al. 2010). While limited site-to-site variability is observed in Ecuador (when considering the new estimated values for El Reventador, Cotopaxi and Tungurahua; Tab. 3), a manifest disparity arises from the comparison between He isotope compositions obtained for Ecuadorian volcanoes and those of Colombia with significantly higher $^3He/^4He$ ratios (Fig. 4). In the following sections, we attempt at identifying the causal mechanisms driving the isotopic differences between the two arc regions.

Subduction-related controls on the noble gas chemistry of NVZ fluids

We initially explore a possible link between noble gas compositions and processes occurring within the slab. In other volcanic arcs, such as the Central America Volcanic Arc (CAVA), pronounced along-arc variations in volcanic rock Ba/La ratios, for example within the Nicaraguan segment (Carr, 1984; Protti et al., 1995), coincide with changes in the dipping of the subducting slab, whereby the steepest dip sections induce intensive metasomatism and melting of a smaller volume of mantle (Carr et al., 1990). As a result, melts generated in this region are heavily imprinted with the signature of the subducted slab (e.g., high Ba/La). It is also suggested that local anomalous OIB-like signatures in the CAVA volcanic front are derived from the interaction of the mantle wedge with the Cocos aseismic ridge, the Galapagos Hostpot track, subducting beneath the arc (Benjamin et al., 2007, Hoernle et al., 2008, Wegner et al., 2010; Gazel et al., 2010;). Abratis and Wörner (2001) proposed that a “slab window” in the subducting Cocos Plate (Johnston and Thorkelson, 1997) allows a Galapagos-modified asthenosphere to flow into the Central American subduction system, which may culminate in the high $^3He/^4He$ ratios (as high as 8.9 R_A in Guatemala; Battaglia et al., 2019) previously reported along CAVA (see also Shaw et al., 2003; Tassi et al., 2004; Shaw et al., 2006; Di Piazza et al., 2015; Rizzo et al., 2016; Robidoux et al., 2017; Battaglia et al., 2018).

Similarly, Bryant et al. (2006) reported relatively primitive isotopic signatures (e.g., Pb and Nd) for Ecuadorian lavas. These isotope compositions, as reported, appear largely independent on their major elements and on the age or composition of the crust through which they were erupted. Moreover, they partially overlap the range of Galapagos Plume basalts (Bryant et al., 2006). Ancellin et al. (2017, 2019) described similar evidence for the interaction between melts from the subducting Carnegie Ridge (Galapagos Plume track) and the mantle wedge in the northern Andean volcanic zone in Ecuador. A further role of the slab in the region may manifest in a northward increasing input of C-rich fluids from slab sediment decarbonation (Marín-Cerón et al., 2010), which may well explain the higher CO_2/S_T ratios found in volcanic gases from Galeras and Nevado del Ruiz volcanoes (Aiuppa et al., 2017 and 2019; Lages et al., 2019; Fig. 4), as well as the higher Ba/La averages in Colombian rocks (e.g., Nevado del Ruiz up to ~62) relative to the Ecuadorian volcanoes here studied (Fig. 4). Fluid-mobile (e.g., B, Pb, Sr and Li) and -immobile (e.g., Nb and La) element ratios have also been used to distinguish between dehydration (low temperature) or melting (high temperature) processes of the basaltic oceanic crust and their relative contribution to the nature of the slab components identified along the NVZ (e.g., Marín-Cerón et al., 2010; Samaniego et al., 2010; Narvaez et al., 2018). Interestingly, whether due to changes in the slab component (e.g., Marín-Cerón et al., 2010; Ancellin et al., 2017; Narvaez et al., 2018) or to increasing average depths of arc magma evolution within the overriding plate crust (as argued by Chiaradia et al., 2020 due to effect of the subduction of the Carnegie aseismic ridge), magma chemistry seems to vary significantly along the NVZ.

If gas and rock chemistry data (Fig. 4) point to increasing fractions of slab fluids toward the north, our results, on the other hand, do not echo that same along-segment variability. Slab sediment fluids and melts are effective U and Th carriers (e.g., Kelley et al., 2005), so the injection of a slab component should contribute significant amounts of radiogenic ^{4}He into the overriding mantle wedge, thus lowering its ^{3}He/^{4}He ratio. If the addition of slab sediment was the primary driver of along-arc noble gas isotope variations, then lower ^{3}He/^{4}He ratios should in principle be observed in Colombia. In contrast, our results imply an Ecuador average of ~7.2 R_A (Cotopaxi, Tungurahua and Reventador maximum ^{3}He/^{4}He values of 7.0, 7.0 and 7.4 R_A, respectively; maximum R_C/R_A ratios obtained for each volcano are taken into account as their primitive/magmatic "end-member"), whereas FIs from Nevado del Ruiz (~8.5 R_A) and fumarolic gases from Galeras (8.8 R_A, from Sano et al., 1997; and 8.3 R_A from this study) all show significantly higher R_C/R_A ratios (>1 R_A unit; Tab. 1).

In summary, although changes in subduction-related parameters (e.g., slab angle and slab descent rate; see Syracuse and Abers, 2006) and in slab thermal regime (due to the presence of the subducted Carnegie ridge; Syracuse et al., 2010; Yepes et al. 2016; Narvaez et al., 2018) appear key to generating the chemical/isotopic (Sr, Nd, Pb) diversity of NVZ magmas, they do not seem to be the main drivers of helium isotopic variations in magmatic fluids registered here. More broadly, the ≤8.5 R_A ratios observed here indicate a negligible contribution of hot-spot-related fluids (measured up to ~18 R_A in the Galapagos; see Goff et al., 2000), and indicate that a variable extent of crustal fluid-addition to primary (mantle-derived) melts may be the governing process as to explain the He isotope difference between Ecuador and Colombia.

6.3. Crustal assimilation of radiogenic ^{4}He

As previously discussed, ^{3}He/^{4}He values recorded in orthopyroxenes from Cotopaxi (<< 8 R_A) seem to be linked to processes of isotope fractionation and extensive helium loss. However, apart from this sample, all ^{3}He/^{4}He ratios in phenocrysts and fumarolic gases reported (Tab. 1 and 2) are significantly higher than orthopyroxenes from Cotopaxi, with most samples lying approximately within MORB range (8 ± 1 R_A). The notable exceptions here are the olivine phenocrysts from Galeras A and B, both yielding slightly lower-than MORB R_C/R_A ratios. This is even more emphasized by the discrepancy between the R_A values reported in olivine inclusions and those of fumarolic gases sampled at the central crater in July 2017 (8.3 ± 0.1 and 8.2 ± 0.1 R_A; see Tab. 2 and Fig. 4) and reported by Sano et al. (1997) between 1988-1993 (as high as 8.8 ± 0.6 R_A). Another important observation from our newly reported dataset is that averaged ^{3}He/^{4}He isotope values for Ecuador and Colombia, calculated by considering the highest measured ^{3}He/^{4}He (R_C/R_A) ratio for each volcano (from fluid inclusions or free gases), differ by 1.5 R_A units (Ecuador ~7.2 R_A; Colombia ~8.5 R_A).

Compositional and isotope variations recorded in magmatic fluids can be explained through multiple contributions that, in addition to the mantle and the subducted slab, include fluids derived from the continental crust (e.g., Garrison et al., 2011; Nauret et al., 2018). Interestingly, models of crustal thickness for the continental Andes (e.g., Assumpção et al., 2013) reveal significant along-arc variations. Bryant et al. (2006) reported a very thick crust (≥50 km) underlying the currently active volcanic arc in Ecuador (e.g., Moho depths of ~53 km under Cotopaxi volcano; Bishop et al., 2017; see Vaca et al., 2019 for more detail information). In Colombia gravity data showed the thickness of the crust for this region to be between 30-40 km (e.g., Mooney et al.,1998; Ojeda and Havskov, 2001). Schaefer (1995) found a thin crust (<35 km) and/or an anomalous dense crust around the Nevado del Ruiz (Fig. 5A).

According to most authors, NVZ magmas appear to be contaminated to a greater extent in the lower crust (Garrison et al., 2011; Bryant et al., 2006; Ancellin et al., 2017; Nauret et al., 2018). Nonetheless, previous works (Barragan et al., 1998; Bourdon et al., 2003; Bryant et al., 2006; Samaniego et al., 2005; Chiaradia et al., 2011; Hidalgo et al., 2012; Ancellin et al., 2017, 2019; Nauret et al., 2018) also estimated the amount of upper crustal contamination in Ecuadorian magmas (using different tools such as trace elements and Sr-Nd-O isotopes) to be 7 to 14 vol % in the Western Cordillera and 6 to 13 vol % in the Eastern Cordillera. In fact, partial or bulk assimilation of crustal lithologies by basaltic-andesite magmas is an intuitively reasonable and thermodynamically possible explanation for the chemistry of these magmas (e.g., Kerr et al., 1995), especially those extruding in arc regions characterized by exceptionally thick continental crust, such as the Ecuadorian arc (≥50 km) and southernmost regions of Colombia (45-50 km; Feininger and Seguin, 1983; Prévot et al., 1996; Guillier et al., 2001). The link between crustal thickness and magma composition (Leeman, 1983; Plank and Langmuir, 1988) may be the driver for the formation of more evolved eruptive products, as those seen throughout the Northern Volcanic Zone. Some of these rocks were investigated by James and Murcia (1984) for Galeras and Nevado del Ruiz (Colombia), that found isotopic evidence for significant ^{18}O-rich crustal components in the petrogenesis of these eruptive products, mostly related to processes happening during magmatic ascent. The lack of basalts in this part of the arc also suggests assimilation and/or magma mixing process of crustal materials by mantle-derived arc-magmas (Marín-Cerón et al., 2010).

Despite the recognition of crustal processes as key drivers of magma evolution in the NVZ, it is assumed that they do not overprint slab and mantle signatures in Ecuador and have overall little effect on Sr-Nd-O isotope systematics and trace elements of magmas erupted in the region (e.g., Barragan et al., 1998; Hidalgo et al., 2012; Ancellin et al., 2017). Our isotope systematics, on the other hand, confirm that shallow (crustal) noble gas imprint is significant in the area, and key to explaining the helium isotope signature differences between Ecuador and Colombia. The extent of fluid contamination by radiogenic crustal components can vary substantially depending on a wide range of geochemical and geophysical parameters. We propose that fluids trapped in olivine from Ecuadorian volcanoes, yielding lower limit-MORB range $^3He/^4He$ isotope signatures (avg. 7.2 R_A), may reflect crustal assimilation of deep magmatic fluids, slowly ascending to shallower sub-reservoir levels, especially along the main volcanic arc where crustal thickness is reported to be ≥50 km. Furthermore, basement below Cotopaxi, Tungurahua and Reventador correspond to mature lithologies, which might enhance the role of crustal contamination and hence reduce the $^3He/^4He$ ratios of magmatic fluids. Given the high U and Th contents of lower and upper crust materials (0.2 and 1.2 ppm, to 2.7 and 10.5 ppm, respectively; Rudnick and Fountain, 1995; Rudnick and Gao, 2003, 2014; see also Hacker et al., 2011), we argue that noble gas isotope compositions, especially helium, in the NVZ may well be impacted by (and be suitable tracers of) shallow crustal assimilation processes, either related to stationary magma bodies (magma aging) and/or interaction of fluids with crustal rocks. We therefore suggest that crustal processes play a crucial role in controlling to lower the $^3He/^4He$ isotope compositions (at the lower MORB range) in Ecuadorian samples, at least in comparison to the higher R_C/R_A values seen in phenocrysts from Nevado del Ruiz and measured in fumarolic gases at Galeras.

If contamination of pristine noble gas compositions is essentially occurring in the crust, as our data seem to support, it is therefore plausible to suggest a homogenous noble gas signature to the mantle source beneath the NVZ. Perhaps, an inefficient slab transport of light noble gases (He, Ne, Ar) in sub-arc regions, due to early (in the trench) devolatilization of these gases, may lead to a relatively homogeneous, MORB-type mantle wedge. Previous studies have relied heavily on $^{13}C/^{12}C$ and $CO_2/^3He$ to constrain mixing of marine limestones and organic sediments with upper mantle fluids (e.g., Marty and Jambon, 1987; Sano and Marty, 1995; and references therein). Although we were unable to estimate the $\delta^{13}C$ of individual samples (due to the CO_2-poor nature of FIs analyzed), our study reports on the first CO_2 concentrations in FIs from arc volcanism. From these, we find $CO_2/^3He$ ratios in the Ecuadorian samples that suggest early exsolution of CO_2 from the magma, and subsequent entrapment of CO_2-depleted fluids by crystals forming at shallow depths with variable extents of crustal contamination (Fig. 5B). Notably, $CO_2/^3He$ measured in FIs of Galeras reflect greater outgassing than those of surface fumaroles with $^3He/^4He$ ratios in the range of Nevado del Ruiz FIs results. Else, we suggest that the slight increase in $CO_2/^3He$ ratios in olivines from El Reventador, Cotopaxi and Tungurahua (as high as 6.1×10^9 in olivine phenocrysts from El Reventador lavas) may reflect higher degrees of crustal outgassing. This is consistent with the lower Ecuadorian $^3He/^4He$ "end-member" that point to assimilation of radiogenic ^4He from the surrounding crust during magma storage in the thicker continental crust.

7. Concluding remarks

Processes of magmatic fluids ascent and consequent interactions with continental crust make volcanic arcs a challenging geodynamic setting when it comes to characterizing the pristine noble gas composition of upper mantle fluids feeding volatiles, including noble gases, to shallower magmatic reservoirs. In regions of thick crust, like the Andes, such task becomes increasingly difficult, with rare petrogenetic examples of uncontaminated mantle products rising to the Earth's surface. Depending of the isotopic system used, the amount of the crustal imprint is different, the challenge being to resemble all the different (and intrinsically incomplete) perspectives into a more complete view of the evolutionary stages of arc magmas and their inherited isotopic signatures.

New noble gas data reported here for FIs hosted in olivine and orthopyroxene phenocrysts from 5 of the most active volcanoes in the Northern Volcanic Zone, and updated fumarolic isotope compositions for Galeras, have allowed us to characterize the noble gas signatures of deep fluids along the northernmost segment of the Andean Volcanic Belt, with the following important conclusions:

1. New He isotope data reported for the Ecuadorian arc, and first helium isotope characterization of eruptive products from Reventador, Cotopaxi and Tungurahua (for which only peripheral, low-temperature data had yet been reported) revealed significantly higher helium isotope signatures (Avg. R_C/R_A ~7.2) than those previously reported in literature (max. 6.8 and 5.1 R_A for Cotopaxi and Tungurahua, respectively; Inguaggiato et al., 2010).

2. The highest $^3He/^4He$ ratio measured in rocks and gases for each individual volcanic system (7.0–8.5 R_A) are consistent with the typical MORB-range expected for arc volcanism (8 ± 1 R_A). Excluding Galeras, for which in previous studies R_C/R_A values reached up to ~8.8 R_A, all values obtained in this study represent the highest R_C/R_A values reported to date on these volcanic systems.

3. A significant discrepancy arises when averaging the highest $^3He/^4He$ from individual volcanic centers from the two arc segments, with an estimated average of ~7.2 R_A for Ecuador and ~8.5 R_A for Colombia. Although the reported constrains fall within the expected MORB range, we argue that a systematic difference exists between the two NVZ regions.

4. Whole rock chemistry (e.g., Ba/La, La/Yb) from lavas and other eruptive products show significant N-S variation in trace element signatures that can either be explained by changes in the slab component or

variations in the average depth of evolution of arc magmas within the NVZ crust. However, noble gas isotope systematics, especially $^3He/^4He$ ratios, show little intra-segment variability within both Ecuador and Colombia.

5. Instead, while comparing the two arc segments (between Colombia and Ecuador), a positive correlation is observed between thickness of the overlying of continental crust and helium isotope signature, suggesting that noble gas compositions are likely controlled by shallower addition of crustal (radiogenic) ^4He whether as gas percolates through the host rock, or by assimilation of U-Th-rich crustal lithologies as magma reservoirs interact with the host rock. The first CO_2 concentration measurements in FIs from Andean volcanoes, integrated with noble gases, support this interpretation.

6. We therefore suggest a rather homogeneous, MORB-like helium isotopic signature to the mantle underlying the active volcanism along the arc segments of Colombia and Ecuador (Northern Volcanic Zone).

In summary, this study brings significant contribution to our knowledge of noble gas circulation and crustal assimilation processes happening at arc segments of exceptionally thick continental crust. Our results underline the sensitivity of He in identifying and assessing crustal contamination processes at volcanic arc settings. We also demonstrate the importance of using FIs to constrain $^3He/^4He$ mantle/magma signatures, the message from surface gases being more subtle and difficult to interpret. In order to better constrain volatile source/behavior at arcs and understand the possible role of slab geometry along the Northern Volcanic Zone, future studies must concentrate on establishing a much more systematic approach to sampling of noble gases and expanding current datasets.

Declaration of competing interest

The authors declare that they have no known competing financial interests or personal relationships that could have appeared to influence the work reported in this paper.

Acknowledgements

This research was conducted as part of Joao Lages Ph.D. research which was financially supported by the *Università degli Studi di Palermo*. The Ecuador portion of this investigation was conducted as part of the "Trail by Fire" project (P.I. Moussallam, Y.). We would like to acknowledge all the staff members from the *Instituto Geofísico — Escuela Politécnica Nacional,* (Quito, Ecuador) for their incredible logistical and technical support throughout our field campaign (February 2017). Special thanks to Dr. Benjamin Bernard for his assistance and scientific advice, and for providing the rock samples from Reventador analyzed in this study. We would also like to thank the *Servicio Geológico Colombiano*, the volcanological observatories of Pasto and Manizales, and their staff, for their crucial assistance with fieldwork in Galeras and Nevado del Ruiz. INGV-Palermo provided the analytical facilities and we would also like to thank their staff members Mariano Tantillo and Mariagrazia Misseri for their support in sample preparation and noble gases analysis of FIs. The fieldwork portion of this work was funded by the DECADE initiative, from Deep Carbon Observatory - Alfred P. Sloan Foundation and by the Royal Geographical Society (with the Institute of British Geographers) with the Land Rover Bursary. A.A. and A.L.R. also received funding from the MIUR (under grant PRIN2017 - 2017LMNLAW).

References

Abratis, M., Wörner, G., 2001. Ridge collision, slab-window formation, and the flux of Pacific asthenosphere into the Caribbean realm. Geology 29, 127–130. https://doi.org/10.1130/0091-7613(2001)029<0127:RCSWFA>2.0.CO;2

Aguilera, E., Almeida, E., Balseca, W., Barberi, F., Innocenti, F., Coltelli, M., Pasquare, G., 1988. El Reventador: an active volcano in the sub-andean zone of Ecuador. Rendiconti della Societa Italiana di Mineralogia e Petrologia 43, 853–875.

Aguilera, F., Tassi, F., Darrah, T., Moune, S., Vaselli, O., 2012. Geochemical model of a magmatic–hydrothermal system at the Lastarria volcano, northern Chile. Bulletin of volcanology 74(1), 119-134. https://doi.org/10.1007/s00445-011-0489-5

Aiuppa, A., Fischer, T.P., Plank, T., Bani, P., 2019. CO_2 flux emissions from the Earth's most actively degassing volcanoes, 2005–2015. Sci. Rep. 9, 2005–2015. https://doi.org/10.1038/s41598-019-41901-y

Aiuppa, A., Fischer, T.P., Plank, T., Robidoux, P., Di Napoli, R., 2017. Along-arc, inter-arc and arc-to-arc variations in volcanic gas CO_2/S_T ratios reveal dual source of carbon in arc volcanism. Earth-Science Rev. 168, 24–47. https://doi.org/10.1016/j.earscirev.2017.03.005

Allègre, C.J., Staudacher, T., Sarda, P., 1987. Rare gas systematics: formation of the atmosphere, evolution and structure of the Earth's mantle. Earth Planet. Sci. Lett. 81, 127–150. https://doi.org/10.1016/0012-821X(87)90151-8

Ancellin, M-A., Samaniego, P., Vlastelic, I., Nauret, F., Gannoun, A., Hidalgo, S., 2017. Across-arc versus along-arc Sr-Nd-Pb isotope variations in the Ecuadorian volcanic arc. Geochemistry Geophysics, Geosystems, 1–26. https://doi.org/10.1002/2016GC006679.Received

Ancellin, M-A., Vlastélic, I., Samaniego, P., Nauret, F., Gannoun, A., Hidalgo, S., 2019. Up to 1% Pb isotope disequilibrium between minerals hosted in dacites from the Guagua Pichincha volcano, Ecuador: Implication for tracing the source and crustal history of continental arc magmas. Chem. Geol. 525, 177–189. https://doi.org/10.1016/j.chemgeo.2019.07.016

Annen, C., Blundy, J.D., Sparks, R.S.J., 2006. The genesis of intermediate and silicic magmas in deep crustal hot zones. J. Petrol. 47, 505–539. https://doi.org/10.1093/petrology/egi084

Assumpção, M., Feng, M., Tassara, A., Julià, J., 2013. Models of crustal thickness for South America from seismic refraction, receiver functions and surface wave tomography. Tectonophysics 609, 82–96. https://doi.org/10.1016/j.tecto.2012.11.014

Ballentine, C.J., Burgess, R., Marty, B., 2002. Tracing fluid origin, transport and interaction in the crust. Rev. Mineral. Geochemistry 47, 539–614. https://doi.org/10.2138/rmg.2002.47.13

Ballentine, C.J., Marty, B., Lollar, B.S., Cassidy, M., 2005. Neon isotopes constrain convection and volatile origin in the Earth's mantle. Nature 433, 33–38. https://doi.org/10.1038/nature03182

Barazangi, M., Isacks, B.L., 1979. Subduction of the Nazca plate beneath Peru: evidence from spatial distribution of earthquakes. Geophys. J. R. Astron. Soc. 57, 537–555. https://doi.org/10.1111/j.1365-246X.1979.tb06778.x

Barragan, R., Geist, D., Hall, M., Larson, P., Kurz, M., 1998. Subduction controls on the compositions of lavas from the Ecuadorian Andes. Earth Planet. Sci. Lett. 154, 153–166. https://doi.org/10.1016/s0012-821x(97)00141-6

Battaglia, A., Bitetto, M., Aiuppa, A., Rizzo, A.L., Chigna, G., Watson, I.M., D'Aleo, R., Juárez Cacao, F.J., de Moor, M.J., 2018. The magmatic gas signature of Pacaya Volcano, with implications for the volcanic CO_2 flux from Guatemala. Geochemistry, Geophys. Geosystems 19, 667–692. https://doi.org/10.1002/2017GC007238

Benavente, O., Tassi, F., Reich, M., Aguilera, F., Capecchiacci, F., Gutiérrez, F., Vaselli, O., Rizzo, A., 2016. Chemical and isotopic features of cold and thermal fluids discharged in the Southern Volcanic Zone between 32.5 S and 36 S: Insights into the physical and chemical processes controlling fluid geochemistry in geothermal systems of Central Chile. Chemical geology, 420, 97-113. https://doi.org/10.1016/j.chemgeo.2015.11.010

Benjamin, E.R., Plank, T., Wade, J.A., Kelley, K.A., Haun, E.H., Alvarado, G.E., 2007. High water contents in basaltic magmas from Irazu Volcano, Costa Rica. J. of Volcanol. And Geotherm. Res. 168, 68-92. https://doi.org/10.1016/j.jvolgeores.2007.08.008

Bijwaard, H., Spakman, W., Engdahl, E.R., 1998. Closing the gap between regional and global travel time tomography. J. Geophys. Res. Solid Earth 103, 30,055–30,078. https://doi.org/10.1029/98jb02467

Bishop, J.W., Lees, J.M., Ruiz, M.C., 2017. Receiver function stacks: initial steps for seismic imaging of Cotopaxi volcano, Ecuador. In AGU Fall meeting, Abstract 31.

Boudoire, G., Rizzo, A.L., Arienzo, I., Di Muro, A., 2020. Paroxysmal eruptions tracked by variations of helium isotopes: inferences from Piton de la Fournaise (La Réunion island). Scientific Reports, 10:9809. https://doi.org/10.1038/s41598-020-66260-x

Boudoire, G., Rizzo, A.L., Di Muro, A., Grassa, F., Liuzzo, M., 2018. Extensive CO_2 degassing in the upper mantle beneath oceanic basaltic volcanoes: First insights from Piton de la Fournaise volcano (La Réunion Island). Geochim. Cosmochim. Acta 235, 376–401. https://doi.org/10.1016/j.gca.2018.06.004Bourdon, E., Eissen, J.P., Gutscher, M.A., Monzier, M., Hall, M.L., Cotten, J., 2003. Magmatic response to early aseismic ridge subduction: The Ecuadorian margin case (South America). Earth Planet. Sci. Lett. 205, 123–138. https://doi.org/10.1016/S0012-821X(02)01024-5

Bryant, J.A., Yogodzinski, G.M., Hall, M.L., Lewicki, J.L., Bailey, D.G., 2006. Geochemical constraints on the origin of volcanic rocks from the Andean Northern volcanic zone, Ecuador. J. Petrol. 47, 1147–1175. https://doi.org/10.1093/petrology/egl006

Burnard, P., 2004. Diffusive fractionation of noble gases and helium isotopes during mantle melting. Earth and Planetary Science Letters 220, 287–295. https://doi.org/10.1016/S0012-821X(04)00060-3

Burnard, P., 2013. The noble gases as geochemical tracers, The Noble Gases as Geochemical Tracers. https://doi.org/10.1007/978-3-642-28836-4

Burnard, P., Graham, D., Turner, G., 1997. Vesicle-specific noble gas analyses of “popping rock”: Implications for primordial noble gases in earth. Science, 276, 568–571. https://doi.org/10.1126/science.276.5312.568

Calvache, M.L., 1990. Geology and volcanology of the recent evolution of Galeras volcano, Colombia. M. S Thesis, Louisiana State University.

Calvache V., M.L., Williams, S.N., 1997a. Emplacement and petrological evolution of the andesitic dome of Galeras volcano, 1990-1992. J. Volcanol. Geotherm. Res. 77, 57–69. https://doi.org/10.1016/S0377-0273(96)00086-8

Calvache V., M.L., Williams, S.N., 1997b. Geochemistry and petrology of the Galeras Volcanic Complex, Colombia. J. Volcanol. Geotherm. Res. 77, 21–38. https://doi.org/10.1016/S0377-0273(96)00084-4

Capasso, G., Carapezza, M.L., Federico, C., Inguaggiato, S., Rizzo, A., 2005. Geochemical monitoring of the 2002-2003 eruption at Stromboli volcano (Italy): Precursory changes in the carbon and helium isotopic composition of fumarole gases and thermal waters. Bull. Volcanol. 68, 118–134. https://doi.org/10.1007/s00445-005-0427-5

Caracausi, A., Italiano, F., Paonita, A., Rizzo, A., Nuccio, P.M., 2003. Evidence of deep magma degassing and ascent by geochemistry of peripheral gas emissions at Mount Etna (Italy): Assessment of the magmatic reservoir pressure. J. Geophys. Res. Solid Earth 108, 1–15. https://doi.org/10.1029/2002jb002095

Carr, M.J., Feigenson, M.D., Bennett, E.A., 1990. Incompatible element and isotopic evidence for tectonic control of source mixing and melt extraction along the Central American arc. Contrib. to Mineral. Petrol. 105, 369–380. https://doi.org/10.1007/BF00286825

Carr, M.J., 1984. Symmetrical and segmented variation of physical and geochemical characteristics of the central american volcanic front. J. Volcanol. Geotherm. Res. 20, 231–252. https://doi.org/10.1016/0377-0273(84)90041-6

Carr, M.J., Saginor, I., Alvarado, G.E., Bolge, L.L., Lindsay, F.N., Milidakis, K., Turrin, B.D., Feigenson, M.D., Swisher, C.C., 2007. Element fluxes from the volcanic front of Nicaragua and Costa Rica. Geochemistry, Geophys. Geosystems 8. https://doi.org/10.1029/2006GC001396

Chiaradia, M., Müntener, O., Beate, B., 2011. Enriched basaltic andesites from mid-crustal fractional crystallization, recharge and assimilation (Pilavo Volcano, Western Cordillera of Ecuador). J. Petrol. (6), 1107–1141. https://doi.org/10.1093/ petrology/egr020.

Chiaradia, M., Müntener, O., Beate, B., 2020. Effects of aseismic ridge subduction on the geochemistry of frontal arc magmas. Earth Planet. Sci. Lett. 531, 115984. https://doi.org/10.1016/j.epsl.2019.115984

Craig, H., Lupton, J.E., 1976. Primordial neon, helium, and hydrogen in oceanic basalts. Earth Planet. Sci. Lett. 31, 369–385. https://doi.org/10.1016/0012-821X(76)90118-7

Di Piazza, A., Rizzo, A.L., Barberi, F., Carapezza, M.L., De Astis, G., Romano, C., Sortino, F., 2015. Geochemistry of the mantle source and magma feeding system beneath Turrialba volcano, Costa Rica. Lithos 232, 319–335. https://doi.org/10.1016/j.lithos.2015.07.012

Farley, K.A., Neroda, E., 1998. Noble gases in the Earth's mantle. Annu. Rev. Earth Planet. Sci. 26, 189–218. https://doi.org/10.1146/annurev.earth.26.1.189.

Feigenson, M.D., Carr, M.J., 1986. Positively correlated Nd and Sr isotope ratios of lavas from the Central American volcanic front. Geology 14, 79–92. https://doi.org/10.1130/0091-7613(1986)14<79:PCNASI>2.0.CO;2

Feigenson, M.D., Carr, M.J., Maharaj, S.V., Juliano, S., Bolge, L.L., 2004. Lead isotope composition of Central American volcanoes: Influence of the Galapagos plume. Geochemistry, Geophys. Geosystems 5. https://doi.org/10.1029/2003GC000621

Feininger, T., Seguin, M.K., 1983. Simple Bouguer gravity anomaly field and the inferred crustal structure of continental Ecuador. Geology 11, 40–44. https://doi.org/10.1130/0091-7613(1983)11<40:SBGAFA>2.0.CO;2

Fischer, T.P., Takahata, N., Sano, Y., Sumino, H., Hilton, D.R., 2005. Nitrogen isotopes of the mantle: Insights from mineral separates. Geophys. Res. Lett. 32, L11305. https://doi.org/10.1029/2005GL022792

Fukao, Y., Widiyantoro, S., Obayashi, M., 2001. Stagnant slabs in the upper and lower mantle transition region. Rev. Geophys. 39, 291–323. https://doi.org/10.1029/1999RG000068

Garrison, J.M., Davidson, J.P., Hall, M., Mothes, P., 2011. Geochemistry and petrology of the most recent deposits from Cotopaxi Volcano, Northern Volcanic Zone, Ecuador. J. Petrol. 52, 1641–1678. https://doi.org/10.1093/petrology/egr023

Gautheron, C., Moreira, M., 2002. Helium signature of the subcontinental lithospheric mantle. Earth Planet. Sci. Lett. 199, 39–47. https://doi.org/10.1016/S0012-821X(02)00563-0

Gazel, E., Hoernle, K., Carr, M.J., Herzberg, C., Saginor, I., Bogaard, P. Van Den, Hauff, F., Feigenson, M., Swisher, C., 2011. Plume – subduction interaction in southern Central America: Mantle upwelling and slab melting. Lithos 121, 117–134. https://doi.org/10.1016/j.lithos.2010.10.008

Giggenbach, W.F., Sano, Y., Wakita, H., 1993. Isotopic composition of helium, and CO_2 and CH_4 contents in gases produced along the New Zealand part of a convergent plate boundary. Geochim. Cosmochim. Acta 57, 3427–3455. https://doi.org/10.1016/0016-7037(93)90549-C

Goff, F., McMurtry, G.M., Counce, D., Simac, J.A., Roldán-Manzo, A.R., Hilton, D.R., 2000. Contrasting hydrothermal activity at Sierra Negra and Alcedo volcanoes, Galapagos Archipelago, Ecuador. Bull. Volcanol. 62, 34–52. https://doi.org/10.1007/s004450050289

Graham, D.W., 2002. Noble gas isotope geochemistry of mid-ocean ridge and ocean island basalts: Characterization of mantle source reservoirs. Rev. Mineral. Geochemistry 47, 247–317. https://doi.org/10.2138/rmg.2002.47.8

Graham, D.W., Hanan, B.B., Hémond, C., Blichert-Toft, J., Albarède, F., 2014. Helium isotopic textures in Earth's upper mantle. Geochemistry, Geophys. Geosystems 15, 2048–2074. https://doi.org/10.1002/2014GC005264

Grove, T.L., Elkins-Tanton, L.T., Parman, S.W., Chatterjee, N., Müntener, O., Gaetani, G.A., 2003. Fractional crystallization and mantle-melting controls on calc-alkaline differentiation trends. Contrib. to Mineral. Petrol. 145, 515–533. https://doi.org/10.1007/s00410-003-0448-z

Guillier. B., Chatelain, J.L., Jaillard, E., Yepes, H., Poupinet, G., Fels, J. F., 2001. Seismological evidence on the geometry of the orogenic system in central-northern Ecuador (South America). Geophys. Res. Lett. 28, 3749-3752. https://doi.org/10.1029/2001GL013257

Gurenko, A. A., Hoernle, K. A., Hauff, F., Schmincke, H. U., Han, D., Miura, Y. N., and Kaneoka, I., 2006. Major, trace element and Nd-Sr-Pb-O-He-Ar isotope signatures of shield stage lavas from the central and western Canary Islands: insights into mantle and crustal processes. Chem. Geol. 233, 75–112. https://doi.org/10.1016/j.chemgeo.2006.02.016

Gutscher, M.A., Malavieille, J., Lallemand, S., Collot, J.Y., 1999. Tectonic segmentation of the North Andean margin: Impact of the Carnegie Ridge collision. Earth Planet. Sci. Lett. 168, 255–270. https://doi.org/10.1016/S0012-821X(99)00060-6

Hacker, B.R., Kelemen, P.B., Behn, M.D., 2011. Differentiation of the continental crust by relamination. Earth Planet. Sci. Lett. 307, 501–516. https://doi.org/10.1016/j.epsl.2011.05.024

Hall, M.L., Samaniego, P., Le Pennec, J.L., Johnson, J.B., 2008. Ecuadorian Andes volcanism: A review of Late Pliocene to present activity. J. Volcanol. Geotherm. Res. 176, 1–6. https://doi.org/10.1016/j.jvolgeores.2008.06.012

Hall, M.L, Mothes, P., 2008. The rhyolitic-andesitic eruptive history of Cotopaxi volcano, Ecuador. Bull. Volcanol. 70, 675–702. https://doi.org/10.1007/s00445-007-0161-2

Hall, M.L., Robin, C., Beate, B., Mothes, P., Monzier, M., 1999. Tungurahua Volcano, Ecuador: Structure, eruptive history and hazards. J. Volcanol. Geotherm. Res. 91, 1–21. https://doi.org/10.1016/S0377-0273(99)00047-5

Hart, S.R., 1984. He diffusion in olivine. Earth Planet. Sci. Lett. 70, 297–302. https://doi.org/10.1016/0012-821X(84)90014-1

Harrison, D., Barry, T., and Turner, G., 2004. Possible diffusive fractionation of helium isotopes in olivine and clinopyroxene phenocrysts. Eur. J. Mineral., 16, 213-220. https://doi.org/10.1127/0935-1221/2004/0016-0213

Hauri, E., 2002. SIMS analysis of volatiles in silicate glasses, 2: Isotopes and abundances in Hawaiian melt inclusions. Chem. Geol. 183, 115–141. https://doi.org/10.1016/S0009-2541(01)00374-6

Heier, K.S., Adams, J.A.S., 1965. Concentration of radioactive elements in deep crustal material. Geochimica et Cosmochimica Acta, 29, pp. 53-61. https://doi.org/10.1016/0016-7037(65)90078-5

Hickey, R.L., Frey, F.A., Gerlach, D.C., Lopez-Escobar, L., 1986. Multiple sources for basaltic arc rocks from the southern volcanic zone of the Andes (34°–41°S): Trace element and isotopic evidence for contributions from subducted oceanic crust, mantle, and continental crust. J. Geophys. Res. 91, 5963. https://doi.org/10.1029/jb091ib06p05963

Hidalgo, S., Battaglia, J., Arellano, S., Sierra, D., Bernard, B., Parra, R., Kelly, P., Dinger, F., Barrington, C., Samaniego, P., 2018. Evolution of the 2015 Cotopaxi eruption revealed by combined geochemical and seismic observations. Geochemistry, Geophysics, Geosystems, 19, 2087–2108. https://doi.org/10.1029/ 2018GC007514

Hidalgo, S., Gerbe, M.C., Martin, H., Samaniego, P., Bourdon, E., 2012. Role of crustal and slab components in the Northern Volcanic Zone of the Andes (Ecuador) constrained by Sr-Nd-O isotopes. Lithos 132–133, 180–192. https://doi.org/10.1016/j.lithos.2011.11.019

Hildreth, W., Moorbath, S., 1988. Crustal contributions to arc magmatism in the Andes of Central Chile. Contrib. to Mineral. Petrol. 98, 455–489. https://doi.org/10.1007/BF00372365

Hilton, D.R., Hammerschmidt, K., Teufel, S., Friedrichsen, H., 1993a. Helium isotope characteristics of Andean geothermal fluids and lavas. Earth Planet. Sci. Lett. 120, 265–282. https://doi.org/10.1016/0012-821X(93)90244-4

Hilton, D.R., Fischer, T. P., Marty, B., 2002. Noble Gases and Volatile Recycling at Subduction Zones. Rev. in Mineralogy and Geochemistry 47 (1), 319–370. https://doi.org/10.2138/rmg.2002.47.9

Hoernle, K., Werner, R., Morgan, J.P., Garbe-Schonberg, D., Bryce, J., Mrazek, J., 2000. Existence of complex spatial zonation in the Galapagos plume for at least 14 m.y. Geology 28, 435-438. https://doi.org/10.1130/0091-7613(2000)28<435:EOCSZI>2.0.CO;2

Huang, Y., Chubakov, V., Mantovani, F., Rudnick, R.L., McDonough, W.F., 2013. A reference Earth model for the heat-producing elements and associated geoneutrino flux. Geochem. Geophys. Geosyst. 14, 2003–29. https://doi.org/10.1002/ggge.20129

Hulston, J.R., Hilton, D.R., Kaplan, I.R., 2001. Helium and carbon isotope systematics of natural gases from Taranaki Basin, New Zealand. Appl. Geochemistry 16, 419–436. https://doi.org/10.1016/S0883-2927(00)00045-7

Inguaggiato, S., Hidalgo, S., Beate, B., Bourquin, J., 2010. Geochemical and isotopic characterization of volcanic and geothermal fluids discharged from the Ecuadorian volcanic arc. Geofluids 10, 525–541. https://doi.org/10.1111/j.1468-8123.2010.00315.x

Inguaggiato, S., Londoño, J.M., Chacón, Z., Liotta, M., Gil, E., Alzate, D., 2017. The hydrothermal system of Cerro Machín volcano (Colombia): New magmatic signals observed during 2011–2013. Chem. Geol. 469, 60–68. https://doi.org/10.1016/j.chemgeo.2016.12.020

Jackson, C.R.M., Parman, S.W., Kelley, S.P., Cooper, R.F., 2013. Noble gas transport into the mantle facilitated by high solubility in amphibole. Nat. Geosci. 6, 562–565. https://doi.org/10.1038/ngeo1851

James, D.E., Murcia, L.A., 1984. Crustal contamination in northern Andean volcanics. J. Geol. Soc. London. 141, 823–830. https://doi.org/10.1144/gsjgs.141.5.0823

Jarrard, R.D., 1986. Relations among subduction parameters. Rev. Geophys. 24, 217–284. https://doi.org/10.1029/RG024i002p00217

Johnston, S.T., Thorkelson, D.J., 1997. Cocos–Nazca slab window beneath Central America. Earth and Planetary Science Letters 146, 465–474. https://doi.org/10.1016/S0012-821X(96)00242-7

Jean-Baptiste, P., Allard, P., Fourré, E., Bani, P., Calabrese, S., Aiuppa, A., Gauthier, P.J., Parello, F., Pelletier, B., Garaebiti, E., 2016. Spatial distribution of helium isotopes in volcanic gases and thermal waters along the Vanuatu (New Hebrides) volcanic arc. J. Volcanol. Geotherm. Res. 322, 20–29. https://doi.org/10.1016/j.jvolgeores.2015.09.026

Kaneoka, I., 1983. Noble gas constrains on the layered structure of the mantle. Nature 302, 698–700. https://doi.org/10.1038/302698a0

Kelemen, P.B., Hanghøj, K., Greene, A.R., 2014. One view of the geochemistry of subduction-related magmatic arcs, with an emphasis on primitive andesite and lower crust. The Crust, Treatise on Geochemistry, edited by H. D. Holland and K. K. Turekian, 69–701, Elsevier-Pergamon, Oxford, U.

Kelley, K.A., Plank, T., Farr, L., Ludden, J., Staudigel, H., 2005. Subduction cycling of U, Th, and Pb. Earth Planet. Sci. Lett. 234, 369–383. https://doi.org/10.1016/j.epsl.2005.03.005

Kendrick, E., Bevis, M., Smalley, R., Brooks, B., Vargas, R.B., Lauría, E., Fortes, L.P.S., 2003. The Nazca-South America Euler vector and its rate of change. J. South Am. Earth Sci. 16(2), 125–131. https://doi.org/10.1016/S0895-9811(03)00028-2

Kennedy, B.M., Hiyagon, H., Reynolds, J.H., 1990. Crustal neon: a striking uniformity. Earth Planet. Sci. Lett. 98, 277–286. https://doi.org/10.1016/0012-821X(90)90030-2

Kerr, A.C., Kempton, P.D., Thompson, R.N., 1995. Crustal assimilation during turbulent magma ascent (ATA); new isotopic evidence from the Mull Tertiary lava succession, N. W. Scotland. Contrib. to Mineral. Petrol. 119, 142–154. https://doi.org/10.1007/BF00307277

Kimura, J.I., Kawabata, H., 2015. Geochemistry, Geophysics, Geosystems. Geochemistry Geophys. Geosystems 16, 267–300. https://doi.org/10.1002/2014GC005684.Key

Kobayashi, M., Sumino, H., Nagao, K., Ishimaru, S., Arai, S., Yoshikawa, M., Kawamoto, T., Kumagai, Y., Kobayashi, T., Burgess, R., Ballentine, C.J., 2017. Slab-derived halogens and noble gases illuminate closed system processes controlling volatile element transport into the mantle wedge. Earth Planet. Sci. Lett. 457, 106–116. https://doi.org/10.1016/j.epsl.2016.10.012

Kurz, M.D., Curtice, J., Fornari, D., Geist, D., Moreira, M., 2009. Primitive neon from the center of the Galápagos hotspot. Earth Planet. Sci. Lett. 286, 23–34. https://doi.org/10.1016/j.epsl.2009.06.008

Lages, J., Chacón, Z., Burbano, V., Meza, L., Arellano, S., Liuzzo, M., Giudice, G., Aiuppa, A., Bitetto, M., López, C., 2019. Volcanic Gas Emissions Along the Colombian Arc Segment of the Northern Volcanic Zone (CAS-NVZ): Implications for volcano monitoring and volatile budget of the Andean Volcanic Belt. Geochemistry, Geophys. Geosystems 20, 1–25. https://doi.org/10.1029/2019gc008573

Le Pennec, J.L., Jaya, D., Samaniego, P., Ramón, P., Moreno Yánez, S., Egred, J., van der Plicht, J., 2008. The AD 1300-1700 eruptive periods at Tungurahua volcano, Ecuador, revealed by historical narratives, stratigraphy and radiocarbon dating. J. Volcanol. Geotherm. Res. 176, 70–81. https://doi.org/10.1016/j.jvolgeores.2008.05.019

Lee, C.T.A., Bachmann, O., 2014. How important is the role of crystal fractionation in making intermediate magmas? Insights from Zr and P systematics. Earth Planet. Sci. Lett. 393, 266–274. https://doi.org/10.1016/j.epsl.2014.02.044

Leeman, W.P., 1983. The influence of crustal structure on compositions of subduction-related magmas. J. Volcanol. Geotherm. Res. 18, 561–588. https://doi.org/10.1016/0377-0273(83)90026-4

Lewicki, J.L., Fischer, T., Williams, S.N., 2000. Chemical and isotopic compositions of fluids at Cumbal Volcano, Colombia: Evidence for magmatic contribution. Bull. Volcanol. 62, 347–361. https://doi.org/10.1007/s004450000100

Lopez, T., Aguilera, F., Tassi, F., Maarten de Moor, J., Bobrowski, N., Aiuppa, A., Tamburello, G., Rizzo, A.L., Liuzzo, M., Viveiros, F., Cardellini, C., Silva, C., Fischer, T., Jean-Baptiste, P., Kazayaha, R., Hidalgo, S., Malowany, K., Lucic, G., Bagnato, E., Bergsson, B., Reath, K., Liotta, M., Carn, S., Chiodini, G., 2018. New insights into the magmatic-hydrothermal system and volatile budget of Lastarria volcano, Chile: Integrated results from the 2014 IAVCEI CCVG 12th Volcanic Gas Workshop. Geosphere 14, 983–1007. https://doi.org/10.1130/GES01495.1

Maldonado, L.F.M., Inguaggiato, S., Jaramillo, M.T., Valencia, G.G., Mazot, A., 2017. Volatiles and energy released by Puracé volcano. Bull. Volcanol. 79. https://doi.org/10.1007/s00445-017-1168-y

Marín-Cerón, M.I., Moriguti, T., Makishima, A., Nakamura, E., 2010. Slab decarbonation and CO_2 recycling in the Southwestern Colombian volcanic arc. Geochim. Cosmochim. Acta 74, 1104–1121. https://doi.org/10.1016/j.gca.2009.10.031

Martelli, M., Rizzo, A.L., Renzulli, A., Ridolfi, F., Arienzo, I., Rosciglione, A., 2014. Noble-gas signature of magmas from a heterogeneous mantle wedge: The case of Stromboli volcano (Aeolian Islands, Italy). Chem. Geol. 368, 39–53. https://doi.org/10.1016/j.chemgeo.2014.01.003

Martinez. N., 1932. Las grandes erupciones del Tungurahua de los años 19 16- 1918. Publicaciones del Observatorio Astronomico de Quito. Seccion de Geofisica. Quito (Ecuador).

Martínez, L.M., Valencia, L. G., Ceballos, J.A., Narváez, B.L., Pulgarín, B.A., Correa, A.M., Navarro, S.R., Murcia, H.F., Zuluaga, I., Rueda, J.B., Pardo, N., 2014. Geología y estratigrafía del Complejo Volcánico Nevado del Ruiz. Geología de volcanes, Dirección de Geociencias básicas. Servicio Geologico Colombiano.

Marty, B., 2012. The origins and concentrations of water, carbon, nitrogen and noble gases on Earth. Earth and Planetary Science Letters, Elsevier 313-314, 56-66. https://doi.org/10.1016/j.epsl.2011.10.040

Marty, B., Jambon, A., 1987. C/^{3}He in volatile fluxes from the solid Earth: implications for carbon geodynamics. Earth Planet. Sci. Lett. 83, 16-26. https://doi.org/10.1016/0012-821X(87)90047-1

Marty, B., Jambon, A., Sano, Y., 1989. Helium isotopes and CO_2 in volcanic gases of Japan. Chem. Geol. 76, 25–40. https://doi.org/10.1016/0009-2541(89)90125-3

Marty, B., Ozima, M., 1986. Noble gas distribution in oceanic basalt glasses. Geochimica et Cosmochimica Acta 50, 1093-1097. https://doi.org/10.1016/0016-7037(86)90390-XMason, E., Edmonds, M., Turchyn, A. V, 2017. Remobilization of crustal carbon may dominate volcanic arc emissions Science (80), 290–294. https://doi.org/10.1126/science.aan5049

Michelfelder, G.S., Feeley, T.C., Wilder, A.D., Klemetti, E.W., 2013. Modification of the Continental Crust by Subduction Zone Magmatism and Vice-Versa: Across-Strike Geochemical Variations of Silicic Lavas from Individual Eruptive Centers in the Andean Central Volcanic Zone. Geosciences 3, 633-667. https://doi.org/10.3390/geosciences3040633

Mooney, W.D., Laske, G. and Masters, T.G., 1998. CRUST 5.1: A Global Crust Model at 5 × 5 degrees. J. Geophys. Res. 103, 727–747. https://doi.org/10.1029/97JB02122

Montelli, R., Nolet, G., Dahlen, F.A., Masters, G., 2006. A catalogue of deep mantle plumes: new results from finite frequency tomography. Geochemistry, Geophys. Geosystems 7, Q11007. https://doi.org/10.1029/2006GC001248

Moreira, M., 2013. Noble gas constraints on the origin and evolution of earth's volatiles. Geochem. Perspec. 2, 229–230. https://doi.org/10.7185/geochempersp.2.2

Moreira, M., Blusztajn, J., Curtice, J., Hart, S., Dick, H., Kurz, M.D., 2003. He and Ne isotopes in oceanic crust: Implications for noble gas recycling in the mantle. Earth Planet. Sci. Lett. 216, 635–643. https://doi.org/10.1016/S0012-821X(03)00554-5

Moreira, M., Kunz, J., Allègre, C., 1998. Rare gas systematics in popping rock: Isotopic and elemental compositions in the upper mantle. Science (80) 279, 1178–1181. https://doi.org/10.1126/science.279.5354.1178

Mysen, B.O., Kushiro, I., Nicholls, I.A., Ringwood, A.E., 1974. A possible mantle origin for andesitic magmas: discussion of a paper by Nicholls and Ringwood. Earth Planet. Sci. Lett. 21, 221-229. https://doi.org/10.1016/0012-821X(74)90157-5

Narvaez, D.F., Rose-Koga, E.F., Samaniego, P., Koga, K.T., Hidalgo, S., 2018. Constraining magma sources using primitive olivine-hosted melt inclusions from Puñalica and Sangay volcanoes (Ecuador). Contrib. to Mineral. Petrol. 173, 80. https://doi.org/10.1007/s00410-018-1508-8

Nauret, F., Samaniego, P., Ancellin, M-A., Tournigand, P.-Y., Le Pennec, J.-L., Vlastelic, I., Gannoun, A., Hidalgo, S., Schiano, P., 2018. The genetic relationship between andesites and dacites at Tungurahua volcano, Ecuador. J. Volcanol. Geotherm. Res. 349, 283-297. https://doi.org/10.1016/j.jvolgeores.2017.11.012

Nicholls, I.A., Ringwood, A.E., 1972. Production of silica-saturated tholeiitic magmas in island arcs. Earth Planet. Sci. Lett. 17, 243–246. https://doi.org/10.1016/0012-821X(72)90282-8

Nocquet, J.M., Villegas-Lanza, J.C., Chlieh, M., Mothes, P.A., Rolandone, F., Jarrin, P., Cisneros, D., Alvarado, A., Audin, L., Bondoux, F., Martin, X., Font, Y., Régnier, M., Vallée, M., Tran, T., Beauval, C., Maguiña Mendoza, J.M., Martinez, W., Tavera, H., Yepes, H., 2014. Motion of continental slivers and creeping subduction in the northern Andes. Nat. Geosci. 7, 287–291. https://doi.org/10.1038/ngeo2099

Notsu, K., Nakai, S., Igarashi, G., Ishibashi, J., Mori, T., Suzuki, M., Wakita, H., 2001. Spatial distribution and temporal variation of 3He/4He in hot spring gas released from Unzen volcanic area, Japan. J. Volcanol. Geotherm. Res. 111, 89–98. https://doi.org/10.1016/S0377-0273(01)00221-9

Ojeda, A., Havskov, J., 2001. Crustal structure and local seismicity in Colombia. J. Seismol. 5, 575–593. https://doi.org/10.1023/A:1012053206408

Oppenheimer, C., Fischer, T.P., Scaillet, B., 2014. Volcanic Degassing: Process and Impact, 2nd ed, Treatise on Geochemistry: Second Edition. Elsevier Ltd. https://doi.org/10.1016/B978-0-08-095975-7.00304-1

Ozima, M., Igarashi, G., 2000. The primordial noble gases in the Earth: A key constraint on Earth evolution models. Earth Planet. Sci. Lett. 176, 219–232. https://doi.org/10.1016/S0012-821X(00)00005-4

Ozima, M., Podosek, F.A. 1983. Noble Gas Geochemistry, 367. Cambridge, London, New York, New Rochelle, Melbourne, Sydney: Cambridge University Press. https://doi.org/10.1017/S0016756800029587

Ozima, M., Podosek, F.A. 2009. Noble Gases in the Earth. Noble Gas Geochemistry 217–252. https://doi.org/10.1017/cbo9780511545986.009

Panter, K.S., Kyle, P.R., Smellie, J.L., 1997. Petrogenesis of a phonolite-trachyte succession at Mount Sidley, Marie Byrd Land, Antarctica. J. Petrol. 38, 1225–1253. https://doi.org/10.1093/petroj/38.9.1225

Paonita, A., Caracausi, A., Iacono-Marziano, G., Martelli, M., Rizzo, A., 2012. Geochemical evidence for mixing between fluids exsolved at different depths in the magmatic system of Mt Etna (Italy). Geochim. Cosmochim. Acta 84, 380–394. https://doi.org/10.1016/j.gca.2012.01.028

Paonita, A., Caracausi, A., Martelli, M., Rizzo, A.L., 2016. Temporal variations of helium isotopes in volcanic gases quantify pre-eruptive refill and pressurization in magma reservoirs: The Mount Etna case. Geology 44, 499–502. https://doi.org/10.1130/G37807.1

Pennington, W.D., 1981.Subduction of the Eastern Panama Basin and Seismotectonics of Northwestern South America. J. Geophys. Res. 86, 10753-10770. https://doi.org/10.1029/JB086iB11p10753

Plank, T., Langmuir, C.H., 1988. The chemical composition of subducting sediment and its consequences for the crust and mantle. Chemical Geology 145, 325–394. https://doi.org/10.1594/PANGAEA.706145

Pistolesi, M., Rosi, M., Cion, R., Cashman, K. V., Rossotti, A., Aguilera, E., 2011. Physical volcanology of the post-twelfth-century activity at Cotopaxi volcano, Ecuador: Behavior of an andesitic central volcano. Bull. Geol. Soc. Am. 123, 1193–1215. https://doi.org/10.1130/B30301.1

Porcelli, D., Wasserburg, G.J., 1995a. Mass transfer of helium, neon, argon, and xenon through a steady-state upper mantle. Geochim. Cosmochim. Acta 59, 4921–4937. https://doi.org/10.1016/0016-7037(95)00336-3

Porcelli, D., Woolum, D., Cassen, P., 2001. Deep earth rare gases: Initial inventories, capture from the solar nebula, and losses during moon formation. Earth Planet. Sci. Lett. 193, 237–251. https://doi.org/10.1016/S0012-821X(01)00493-9

Prévot, R., Chatelain, J.-L., Guillier, B., Yepes, H., 1996. Tomographie des Andes Équatoriennes: évidence d'une continuité des Andes Centrales. Comptes Rendus l'Académie des Sci. Paris 323, 833–840.

Protti, M., Giiendel, F., Mcnally, K., 1995. Correlation between the age of the subducting Cocos plate and the geometry of the Wadati-Benioff zone under Nicaragua and Costa Rica. Geol. Soc. of America. https://doi.org/10.1130/SPE295-p309

Rama, S.N.I., Hart, S.R., Roedder, E., 1965. Excess radiogenic argon in fluid inclusions. J. Geophys. Res. 70, 509-511. https://doi.org/10.1029/JZ070i002p00509

Reubi, O., Blundy, J., 2009. A dearth of intermediate melts at subduction zone volcanoes and the petrogenesis of arc andesites. Nature 461, 1269–1273. https://doi.org/10.1038/nature08510

Ridolfi, F., Puerini, M., Renzulli, A., Menna, M., Toulkeridis, T., 2008. The magmatic feeding system of El Reventador volcano (Sub-Andean zone, Ecuador) constrained by texture, mineralogy and thermobarometry of the 2002 erupted products. J. Volcanol. Geotherm. Res. 176, 94–106. https://doi.org/10.1016/j.jvolgeores.2008.03.003

Rizzo A.L., Caracausi, A., Favara, R., Martelli, M., Nuccio, P.M., Paonita, A., Rosciglione, A., Paternoster, M., 2006. New insights into magma dynamics during last two eruptions of Mount Etna as inferred by geochemical monitoring from 2002 to 2005. Geochem. Geophys. Geosyst. 7, Q06008. https://doi.org/10.1029/2005GC001175

Rizzo, A.L, Grassa, F., Inguaggiato, S., Liotta, M., Longo, M., Madonia, P., Brusca, L., Capasso, G., Morici, S., Rouwet, D., Vita, F., 2009. Geochemical evaluation of observed changes in volcanic activity during the 2007 eruption at Stromboli (Italy). J. Volcanol. Geot. Res. 182, 246–254. https://doi.org/10.1016/j.jvolgeores.2008.08.004

Rizzo, A.L., Federico, C., Inguaggiato, S., Sollami, A., Tantillo, M., Vita, F., Bellomo, S., Longo, M., Grassa, F., Liuzzo, M., 2015a. The 2014 effusive eruption at Stromboli volcano (Italy): Inferences from soil CO_2 flux and $^3He/^4He$ ratio in thermal waters. Geophys. Res. Lett., 42(7), 2235-2243. https://doi.org/10.1002/2014GL062955

Rizzo, A.L., Barberi, F., Carapezza, M.L., Di Piazza, A., Francalanci, L., Sortino, F., D'Alessandro, W., 2015b. New mafic magma refilling a quiescent volcano: Evidence from He-Ne-Ar isotopes during the 2011–2012 unrest at Santorini, Greece. Geochem. Geophys. Geosyst., 16, 798-814. https://doi.org/10.1002/2014GC005653.

Rizzo, A.L., Caracausi, A., Chavagnac, V., Nomikou, P., Polymenakou, P.N., Mandalakis, M., Kotoulas, G., Magoulas, A., Castillo, A., Lampridou, D., Marusczak, N., Sonke, J.E., 2019. Geochemistry of CO_2-Rich Gases Venting from Submarine Volcanism: the case of Kolumbo (Hellenic Volcanic Arc, Greece). Front. Earth Sci. 7, 60. https://doi.org/10.3389/feart.2019.00060

Rizzo, A.L., Di Piazza, A., de Moor, J.M., Alvarado, G.E., Avard, G., Carapezza, M.L., Mora, M.M., 2016. Eruptive activity at Turrialba volcano (Costa Rica): Inferences from $^3He/^4He$ in fumarole gases and chemistry of the products ejected during 2014 and 2015. Geochem. Geophys. Geosyst., 17, 4478–4494. https://doi.org/10.1002/2016GC006525.

Rizzo, A.L., Pelorosso, B., Coltorti, M., Ntaflos, T., Bonadiman, C., Matusiak-Małek, M., Italiano, F., Bergonzoni, G., 2018. Geochemistry of noble gases and CO_2 in fluid inclusions from lithospheric mantle beneath Wilcza Góra (Lower Silesia, Southwest Poland). Frontiers in Earth Sciences 6, 215. https://doi.org/10.3389/feart.2018.00215.

Robidoux, P., Aiuppa, A., Rotolo, S.G., Rizzo, A.L., Hauri, E.H., Frezzotti, M.L., 2017. Volatile contents of mafic-to-intermediate magmas at San Cristóbal volcano in Nicaragua. Lithos 272–273, 147–163. https://doi.org/10.1016/j.lithos.2016.12.002

Rudnick, R.L., Gao, S., 2013. Composition of the Continental Crust, 2nd ed, Treatise on Geochemistry: Second Edition. Elsevier Ltd. https://doi.org/10.1016/B978-0-08-095975-7.00301-6

Rudnick, R.L., 1995. Nature and composition of the continental crust: a lower crustal perspective. Phys. Earth Planet. Inter. 145, 267–309. https://doi.org/10.1029/95RG01302

Samaniego, P., Eissen, J.P., Le Pennec, J.L., Robin, C., Hall, M.L., Mothes, P., Chavrit, D., Cotten, J., 2008. Pre-eruptive physical conditions of El Reventador volcano (Ecuador) inferred from the petrology of the 2002 and 2004-05 eruptions. J. Volcanol. Geotherm. Res. 176, 82–93. https://doi.org/10.1016/j.jvolgeores.2008.03.004

Samaniego, P., Le Pennec, J.L., Robin, C., Hidalgo, S., 2011. Petrological analysis of the pre-eruptive magmatic process prior to the 2006 explosive eruptions at Tungurahua volcano (Ecuador). J. Volcanol. Geotherm. Res. 199, 69–84. https://doi.org/10.1016/j.jvolgeores.2010.10.010

Samaniego, P., Martin, H., Monzier, M., Robin, C., Fornari, M., Eissen, J.P., Cotten, J., 2005. Temporal evolution of magmatism in the Northern Volcanic Zone of the Andes: The geology and petrology of Cayambe volcanic complex (Ecuador). J. Petrol. 46, 2225–2252. https://doi.org/10.1093/petrology/egi053

Samaniego, P., Robin, C., Chazot, G., Bourdon, E., Cotten, J., 2010. Evolving metasomatic agent in the Northern Andean subduction zone, deduced from magma composition of the long-lived Pichincha volcanic complex (Ecuador). Contrib. to Mineral. Petrol. 160, 239–260. https://doi.org/10.1007/s00410-009-0475-5

Sano, Y., Fischer, T.P., 2013. The analysis and interpretation of noble gases in modern hydrothermal systems. In: Burnard P. (eds) The Noble Gases as Geochemical Tracers. Advances in Isotope Geochemistry. Springer, Berlin, Heidelberg

Sano, Y., Gamo, T., Williams, S.N., 1997. Secular variations of helium and carbon isotopes at Galeras volcano, Colombia. J. Volcanol. Geotherm. Res. 77, 255–265. https://doi.org/10.1016/S0377-0273(96)00098-4

Sano, Y., Hirabayashi, J.I., Oba, T., Gamo, T., 1994. Carbon and helium isotopic ratios at Kusatsu-Shirane Volcano, Japan. Appl. Geochemistry 9, 371–377. https://doi.org/10.1016/0883-2927(94)90059-0

Sano, Y., Kagoshima, T., Takahata, N., Nishio, Y., Roulleau, E., Pinti, D.L., Fischer, T.P., 2015. Ten-year helium anomaly prior to the 2014 Mt Ontake eruption. Sci. Rep. 5, 1–7. https://doi.org/10.1038/srep13069

Sano, Y., Marty, B., 1995. Origin of carbon in fumarolic gas from island arcs. Chem. Geol. 119, 265-274. https://doi.org/10.1016/0009-2541(94)00097-R

Sano, Y., Nakajima, J., 2008. Geographical distribution of $^3He/^4He$ ratios and seismic tomography in Japan. Geochem. J. 42, 51–60. https://doi.org/10.2343/geochemj.42.51

Sano, Y., Nakamura, Y., Wakita, H., Urabe, A., Tominaga, T., 1984. Helium-3 Emission Related to Volcanic Activity Science 224,150-151. https://doi.org/10.1126/science.224.4645.150

Sano, Y., Takahata, N., Seno, T., 2006. Geographical distribution of $^3He/^4He$ ratios in the Chugoku District, Southwestern Japan. Pure Appl. Geophys. 163, 745–757. https://doi.org/10.1007/s00024-006-0035-0

Sano, Y., Wakita, H., 1985a. Geographical distribution of $^3He/^4He$ ratios in Japan: implications for arc tectonics and incipient magmatism. J. Geophys. Res. 90, 8729–8741. https://doi.org/10.1029/JB090iB10p08729

Sang, Y., Wakita, H., 1987. Helium isotopes and heat flow on the ocean floor. Chem. Geol. Isot. Geosci. Sect. 66, 217–226. https://doi.org/10.1016/0168-9622(87)90043-1

Sang, Y., Wakita, H., 1988a. Helium isotope ratio and heat discharge rate in the Hokkaido Island, Northeast Japan. Geochem. J. 22, 293-303. https://doi.org/10.2343/geochemj.22.293

Sano, Y., Wakita, H., Williams, S.N., 1990. Helium-isotope systematics at Nevado del Ruiz volcano, Colombia: implications for the volcanic hydrothermal system. J. Volcanol. Geotherm. Res. 42, 41–52. https://doi.org/10.1016/0377-0273(90)90068-Q

Sano, Y., Williams, S.N., 1996. Fluxes of mantle and subducted carbon along convergent plate boundaries. Geophys. Res. Lett. 23, 2749-2752. https://doi.org/10.1029/96GL02260

Sarda, P., Staudacher, T., Allègre, C.J., 1988. Neon isotopes in submarine basalts. Earth Planet. Sci. Lett. 91, 73–88. https://doi.org/10.1016/0012-821X(88)90152-5

Scarsi, P., 2000. Fractional extraction of helium by crushing of olivine and clinopyroxene phenocrysts: Effects on the $^3He/^4He$ measured ratio. Geochimica et Cosmochimica Acta, 64, 3751–3762. https://doi.org/10.1016/S0016-7037(00)00419-1

Schaefer, S.J., 1995. Nevado del Ruiz Volcano, Colombia: Magmatic System and Evolution, PhD. Thesis, Arizona State University. 147 pp.

Schiano, P., Monzier, M., Eissen, J.P., Martin, H., Koga, K.T., 2010. Simple mixing as the major control of the evolution of volcanic suites in the Ecuadorian Andes. Contrib. to Mineral. Petrol. 160, 297–312. https://doi.org/10.1007/s00410-009-0478-2

Schmidt, M.W., Jagoutz, O., 2017. The global systematics of primitive arc melts. Geochemistry, Geophys. Geosystems 18, 2817–2854. https://doi.org/10.1002/2016GC006699

Shaw, A.M., Hilton, D.R., Fischer, T.P., Walker, J.A., de Leeuw, G.A.M., 2006. Helium isotope variations in mineral separates from Costa Rica and Nicaragua: Assessing crustal contributions, timescale variations and diffusion-related mechanisms. Chem. Geol. 230, 124–139. https://doi.org/10.1016/j.chemgeo.2005.12.003

Shinoara, H., Fukui, K., Kazahaya, K., Saito, G., 2003. Degassing process of Miyakejima volcano: implications of gas emission rate and melt inclusion data. Dev. Volcanol. 5, 147–161. https://doi.org/10.1016/S1871-644X(03)80028-1

Smye, A.J., Jackson, C.R.M., Konrad-Schmolke, M., Hesse, M.A., Parman, S.W., Shuster, D.L., Ballentine, C.J., 2017. Noble gases recycled into the mantle through cold subduction zones. Earth Planet. Sci. Lett. 471, 65–73. https://doi.org/10.1016/j.epsl.2017.04.046

Sobolev, A.V., Chaussidon, M., 1996. H2O concentrations in primary melts from supra-subduction zones and mid-ocean ridges: Implications for H2O storage and recycling in the mantle. Earth Planet. Sci. Lett. 137, 45–55. https://doi.org/10.1016/0012-821x(95)00203-o

Stern, C.R., 2004. Active Andean volcanism: its geologic and tectonic setting. Revista Geológica de Chile 31(2), 161-206. http://dx.doi.org/10.4067/S0716-02082004000200001

Stern, R.J., 2002. Subduction zones. Rev. Geophys. 40(4), 1012. https://doi.org/10.1029/2001RG000108

Stix, J., Zapata, J.A., Calvache, M.L., Cortes, G. P., Fischer, T.P., Gomez, D., Narvaez, L., Ordonez, M., Ortega, A., Torres, R., Williams, S.N., 1993. A model of degassing at Galeras Volcano, Colombia, 1988-1993. Geology 21, 963-967. https://doi.org/10.1130/0091-7613(1993)021<0963:AMODAG>2.3.CO;2

Sturchio, N.C., Williams, S.N., Sano, Y., 1993. The hydrothermal system of Volcán Puracé, Colombia. Bull. Volcanol. 55, 289–296. https://doi.org/10.1007/BF00624356

Syracuse E.M., Abers, G.A., 2006. Global compilation of variations in slab depth beneath arc volcanoes and implications. Geochem. Geophys. Geosyst. 7, Q05017. https://doi.org/10.1029/2005GC001045

Syracuse, E.M., van Keken, P.E., Abers, G.A., Suetsugu, D., Bina, C., Inoue, T., Wiens, D., Jellinek, M., 2010. The global range of subduction zone thermal models. Phys. Earth Planet. Inter. 183, 73–90. https://doi.org/10.1016/j.pepi.2010.02.004

Tassi, F., Vaselli, O., Barboza, V., Fernandez, E., Duarte, E., 2004. Fluid geochemistry and seismic activityin the period 1998-2002 at Turrialba Volcano (Costa Rica). Annals of Geophysics 47, 1501-1511. https://doi.org/10.4401/ag-3355

Tatsumi, Y., 1989. Migration of fluid phases and genesis of basalt magmas in subduction zones. J. Geophys. Res. 94, 4697–4707. https://doi.org/10.1029/JB094iB04p04697

Thouret, J.C., Cantagrel, J.M., Salinas, R., Murcia, A., 1990. Quaternary eruptive history of Nevado del Ruiz (Colombia). J. Volcanol. Geotherm. Res. 41, 225–251. https://doi.org/10.1016/0377-0273(90)90090-3

Trenkamp, R., Kellogg, J.N., Freymueller, J.T., Mora, H.P., 2002. Wide plate margin deformation, southern Central America and northwestern South America, CASA GPS observations. J. South Am. Earth Sci. 15, 157–171. https://doi.org/10.1016/S0895-9811(02)00018-4

Trull, T.W., Kurz, M.D., 1993. Experimental measurements of 3He and 4He mobility in olivine and clinopyroxene at magmatic temperatures. Geochim. Cosmochim. Acta 57, 1313–1324. https://doi.org/10.1016/0016-7037(93)90068-8

Trull, T.W., Kurz, M.D., 1999. Isotopic fractionation accompanying helium diffusion in basaltic glass. J. Mol. Struct. 485–486, 555–567. https://doi.org/10.1016/S0022-2860(99)00057-5

Turner, S.J., Langmuir, C.H., Katz, R.F., Dungan, M.A., Escrig, S., 2016. Parental arc magma compositions dominantly controlled by mantle-wedge thermal structure. Nat. Geosci. 9, 772–776. https://doi.org/10.1038/ngeo2788

Umeda, K., Asamori, K., Ninomiya, A., Kanazawa, S., Oikawa, T., 2007. Multiple lines of evidence for crustal magma storage beneath the Mesozoic crystalline Iide Mountains, northeast Japan. J. Geophys. Res. Solid Earth 112, 1–9. https://doi.org/10.1029/2006JB004590

Vaca, S., Vallée, M., Nocquet, J.M., Alvarado, A., 2019. Active deformation in Ecuador enlightened by a new waveform-based catalog of earthquake focal mechanisms. J. South Am. Earth Sci. 93, 449–461. https://doi.org/10.1016/j.jsames.2019.05.017

van der Hilst R.D., Widiyantoro S., Engdahl, E.R., 1997. Evidence for deep mantle circulation from global tomography. Nature 386, 578-584. https://doi.org/10.1038/386578a0

van Keken, P.E., Ballentine, C.J., 1999. Dynamical models of mantle volatile evolution and the role of phase transitions and temperature-dependent rheology. J. Geophys. Res. Solid Earth 104, 7137–7151. https://doi.org/10.1029/1999jb900003

van Keken, P.E., Hauri, E.H., Ballentine, C.J., 2002. Mantle Mixing: The Generation, Preservation, and Destruction of Chemical Heterogeneity. Annu. Rev. Earth Planet. Sci. 30, 493–525. https://doi.org/10.1146/annurev.earth.30.091201.141236

Vatin-Pérignon, N., Goemans, P., Oliver, R.A., Briqueu, L., Thouret, J.C., Salinas, R., Murcia, A., 1988. Magmatic evolution of the Nevado del Ruiz volcano, Central Cordillera, Colombia: Mineral chemistry and geochemistry. Géodynamique, ORSTOM 3, 163–194.

Van Soest, M.C., Hilton, D.R., Kreulen, R., 1998. Tracing crustal and slab contributions to arc magmatism in the Lesser Antilles island arc using helium and carbon relationships in geothermal fluids. Geochim. Cosmochim. Acta 62, 3323–3335. https://doi.org/10.1016/S0016-7037(98)00241-5

Vatin-Pérignon, N., Goemans, P., Oliver, R.A., Palacio, E.P., 1990. Evaluation of magmatic processes for the products of the Nevado del Ruiz Volcano, Colombia from geochemical and petrological data. J. Volcanol. Geotherm. Res. 41, 153–176. https://doi.org/10.1016/0377-0273(90)90087-V

Wallace, P.J., 2005. Volatiles in subduction zone magmas: Concentrations and fluxes based on melt inclusion and volcanic gas data. J. Volcanol. Geotherm. Res. 140, 217–240. https://doi.org/10.1016/j.jvolgeores.2004.07.023

Weber, M.B.I., Tarney, J., Kempton, P.D., Kent, R.W., 2002. Crustal make-up of the northern Andes: evidence based on deep crustal xenolith suites, Mercaderes, SW Colombia. Tectonophysics, 345, 49–82. https://doi.org/10.1016/S0040-1951(01)00206-2

Wegner, W., Wörner, G., Harmon, R.S., Jicha, B.R., 2011. Magmatic history and evolution of the Central American Land Bridge in Panama since Cretaceous times. GSA Bulletin 123, 703-724. https://doi.org/10.1130/B30109.1

Williams, S.N., Sano, Y., Wakita, H., 1987. Helium-3 emission from Nevado del Ruiz, Colombia. Geophys. Res. Lett. 14, 1035–1038. https://doi.org/10.1029/GL014i010p01035

Yamamoto, J., Nishimura, K., Sugimoto, T., Takemura, K., Takahata, N., Sano, Y., 2009. Diffusive fractionation of noble gases in mantle with magma channels: Origin of low He/Ar in mantle-derived rocks. Earth Planet. Sci. Lett. 280, 167–174. https://doi.org/10.1016/j.epsl.2009.01.029

Yepes, H., Audin, L., Alvarado, A., Beauval, C., Aguilar, J., Font, Y., Cotton, F., 2016. A new view for the geodynamics of Ecuador: implication in seismogenic source definition and seismic hazard assessment. Tectonics 35, 1249–1279. https ://doi.org/10.1002/2015T C0039 41

FIGURE CAPTIONS

Figure 1. A:map showing the four volcanically active segments and volcanic gaps along the Andes (adapted from Stern, 2004). **B:**geological setting of the Northern Volcanic Zone (adapted from Bryant et al., 2006), showing the distribution of Quaternary volcanoes along the main magmatic arc (in light yellow); volcanoes included in this study are highlighted in red. On the upper left corner, arrows indicate the subduction direction of the Nazca and Cocos tectonic plates, overlapped on 50-meter resolution DEM map. **C:** Average dip angle of ~20° for Ecuadorian front arc (Yepes et al., 2016), and crustal thickness data (∼50 km) is the average value proposed for the Ecuador segment (Vaca et al., 2019).

Figure 2. A. $^{3}He/^{4}He$ (R/R_A) vs $^{4}He/^{20}Ne$ data from FIs and free gases (low-temperature and fumarolic gases). New data is shown in larger symbols (triangles are fumarolic gases from Galeras). Smaller triangles are fumarolic data from literature (Galeras, from Sano and Williams, 1996, and Sano et al., 1997; and Nevado del Ruiz, from Williams et al., 1987), whereas small squares represent data from low-temperature springs around Tungurahua and Cotopaxi (Inguaggiato et al., 2010). Note the $^{3}He/^{4}He$ avg. for Ecuador and Colombia are given as end-members for each arc segment. Blue and red curves describe a binary mixing between air (grey star) and a magma source with He-isotope compositions of 7.2 and 8.5 R_A, respectively; and shaded area represents the MORB range (8±1 R_A). **B.** $^{4}He/^{20}Ne$ vs $^{40}Ar/^{36}Ar$ and $^{40}Ar/^{36}Ar$ vs $^{3}He/^{36}Ar$ (inset) describing the general atmosphere-mantle mixing trends of the data reported for FIs and fumarolic gases.

Figure 3. Helium characteristics of cogenetic olivine and orthopyroxene phenocrysts from Ecuador. **A.** He concentrates of pyroxenes are plotted against concentrations in cogenetic olivine; the 1:1 line is shown for reference in both. **B.** $^{3}He/^{4}He$ (R_C/R_A) ratios in orthopyroxene vs cogenetic olivine phenocrysts. Except for Cotopaxi lavas (R_C/R_A ratio in opx ~2.2 R_A), note that $^{3}He/^{4}He$ ratios of olivine are indistinguishable of those obtained in cogenetic orthopyroxenes.

Figure 4. On the left: along-arc whole-rock trace element compositions of lavas from Nevado del Ruiz (Perignon et al., 1988), Galeras (Calvache and Williams, 1997a and b), Reventador (Samaniego et al., 2008), Cotopaxi (Garrison et al., 2011) and Tungurahua (Samaniego et al., 2011); shaded areas represent compositional variations between the lowest and highest value reported in literature for a given trace element ratio. At the bottom CO_2/S_T data is from Aiuppa et al., 2019 (in dark) and Lages et al., 2019 (in white); shaded areas represent the uncertainty associated with each volcanic gas measurement; note that CO_2/S_T values for Ecuador (Aiuppa et al., 2019) are predicted using regional/global relationships between the CO_2/S_T ratio of volcanic gases and whole-rock trace element compositions (e.g., Ba/La). On the right: geostatistical interpolation (kriging, Surfer 13 software) of along-arc $^{3}He/^{4}He$ for all locations reported in table 3; note that only maximum values were considered for each individual coordinate point.

Figure 5A. Maximum R_C/R_A values reported in this study (in dark) and in literature (white symbols) for all five volcanoes. Data for Nevado del Ruiz is from Williams et al., 1987; Galeras is from Sano et al., 1997; Tungurahua and Cotopaxi data is from Inguaggiato et al., 2010. Note that dark yellow (Colombia) and red (Ecuador) dashed indicate R_C/R_A averages calculated using only the single highest value for each volcanic system. **Figure 5B.** Crustal thickness variations along the Northern Volcanic Zone from Schaefer (1995), Prévot et al. (1996), Guillier et al. (2001) and Bryant et al. (2006). Inset: $CO_2/^{3}He$ systematics of NVZ fluids; Crust-mantle binary mixing line (in blue) assumes an R_A of 8.5 (avg. Colombia).

Table 1. Noble gas abundances and isotope ratios of mafic phenocrysts from Colombia and Ecuador (Northern Volcanic Zone – Andean Volcanic Belt)

Table 2. Noble gas compositions of fumarolic gases sampled at the central crater of Galeras, Colombia.

Table 3. Helium isotope data compilation for Northern Volcanic Zone Quaternary volcanoes and hydrothermal areas.

Figures

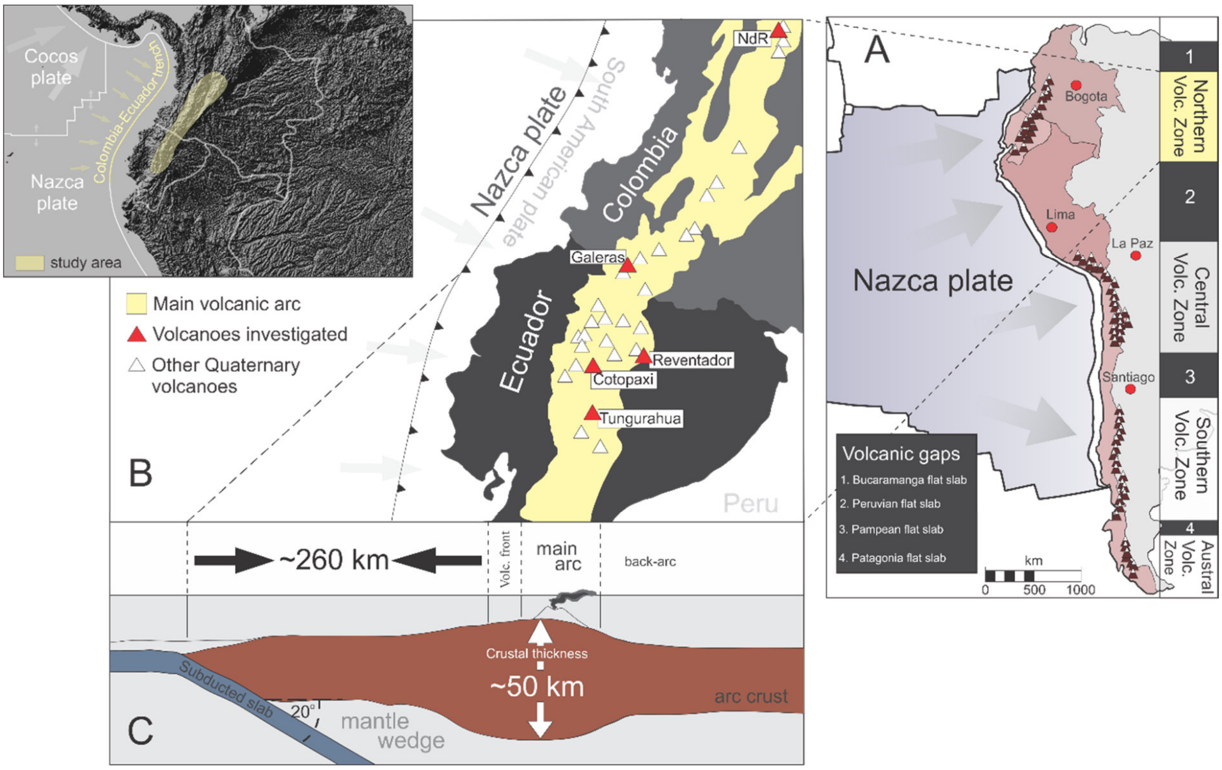

Lages et al. Figure 1

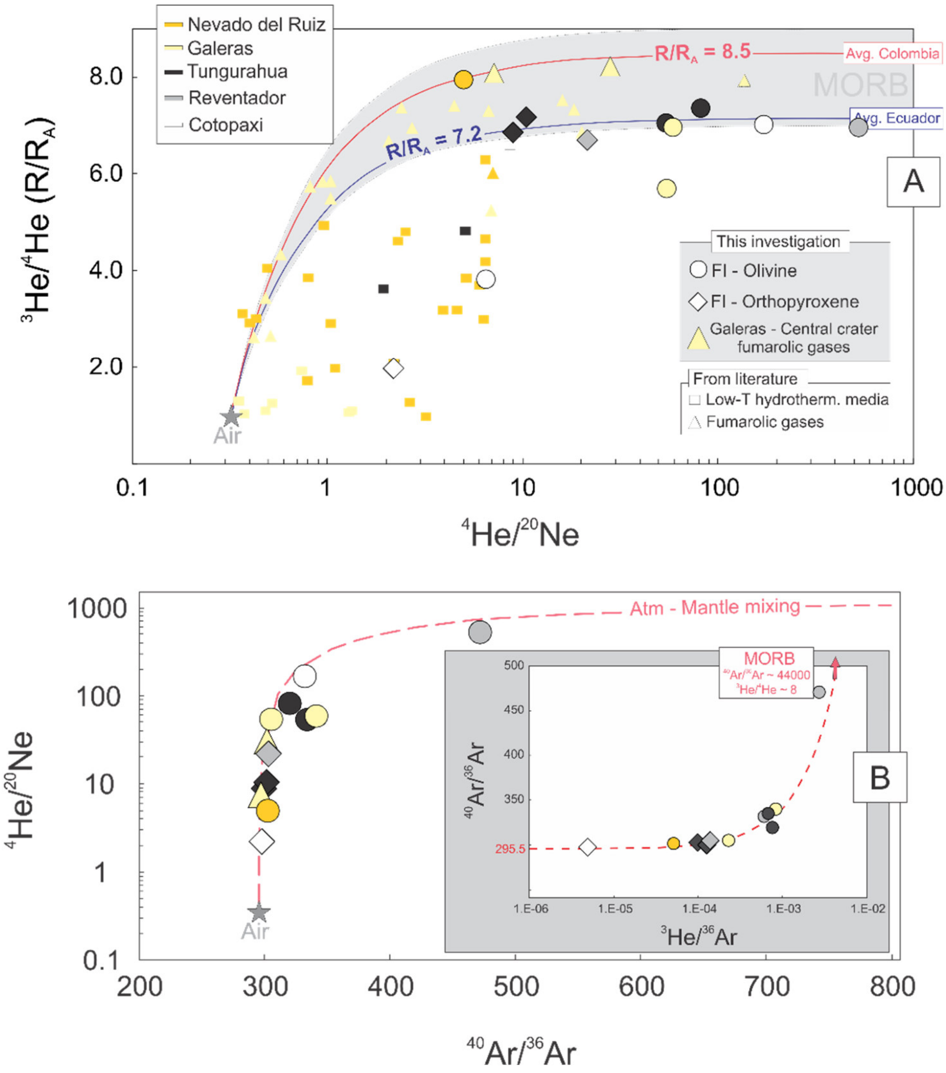

Lages et al. Figure 2

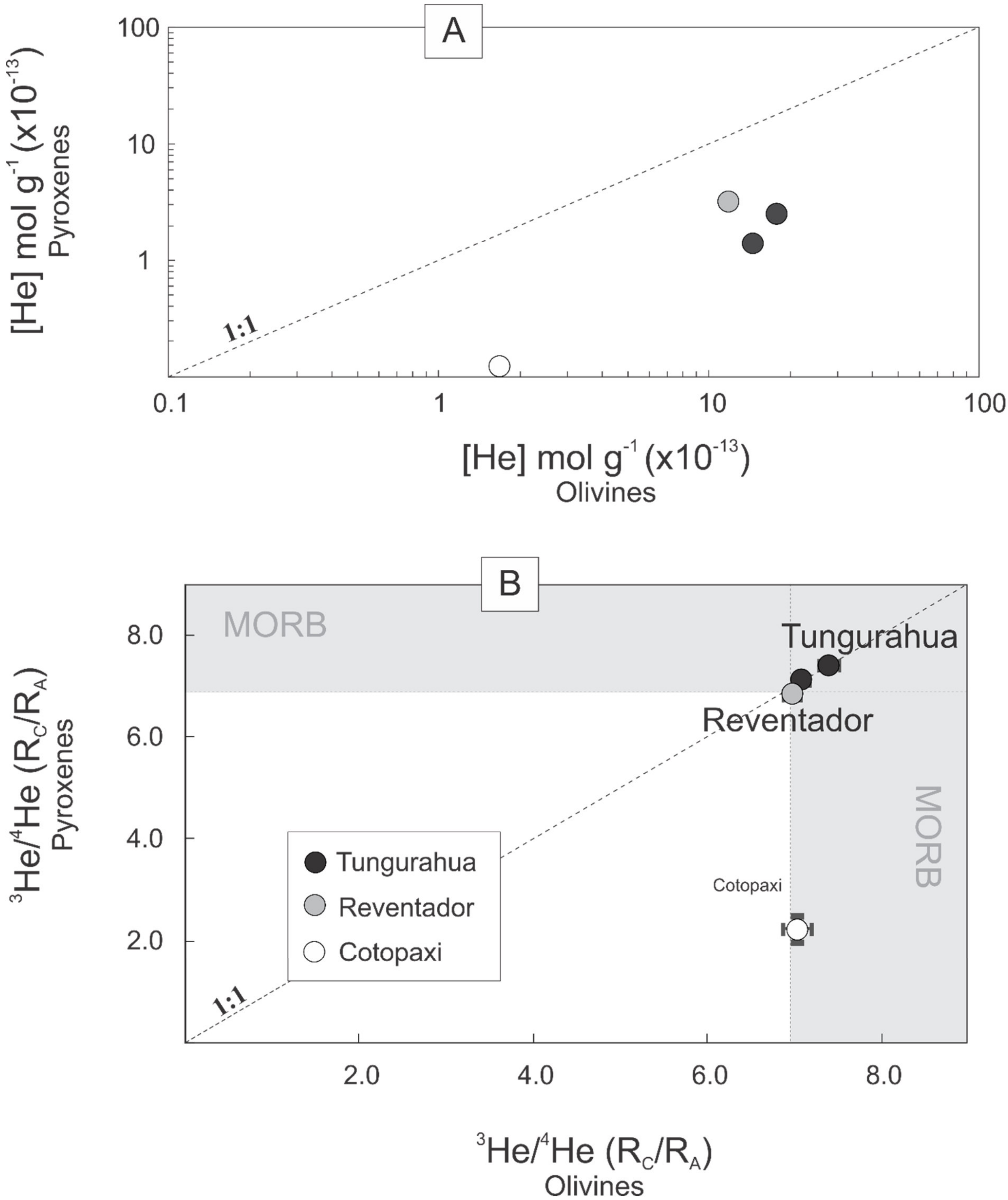

Lages et al., Figure 3

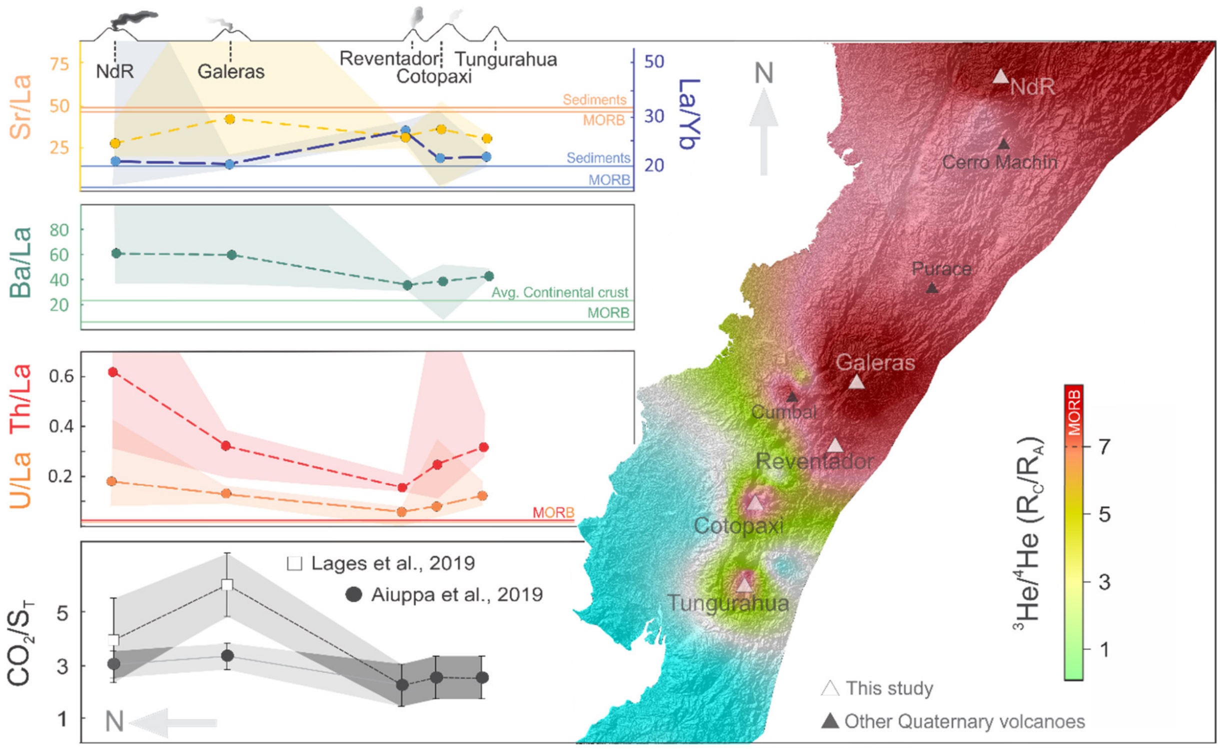

Lages et al. Figure 4

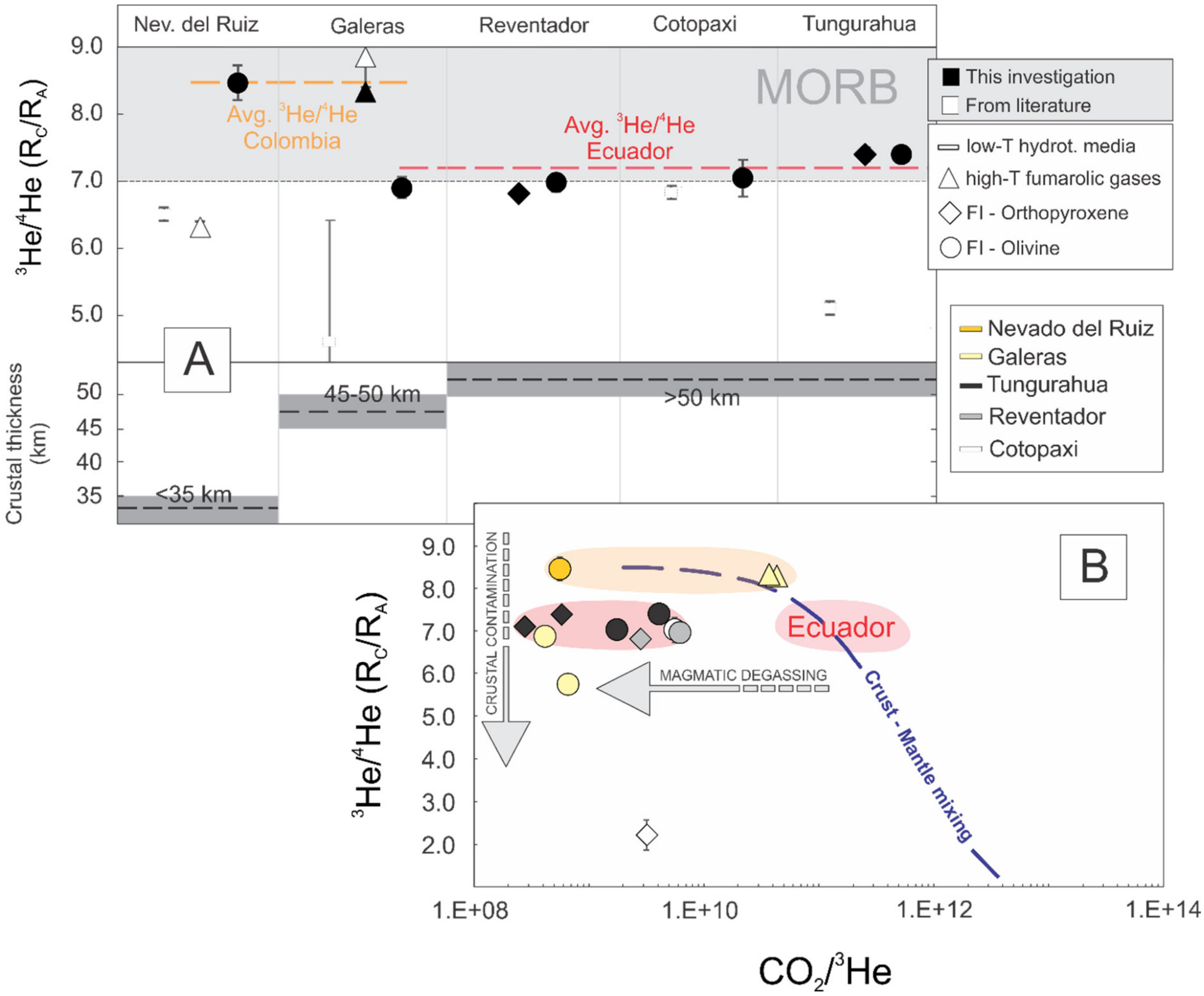

Lages et al. Figure 5

Tables

Table 1
Noble gas abundances and isotope ratios from mafic phenocrysts from Colombia and Ecuador (Northern Volcanic Zone – Andean Volcanic Belt)

Volcano	Sample ID	Sample details	Rock	Min. phase	Weight (g)	[He] $\times10^{-13}$	[Ne] $\times10^{-14}$	[^{40}Ar] $\times10^{-12}$	[^{36}Ar] $\times10^{-15}$	[^{40}Ar*] $\times10^{-13}$	CO_2 $\times10^{-9}$	^{4}He/^{20}Ne	^{20}Ne/^{22}Ne	^{21}Ne/^{22}Ne	He/Ar*	^{40}Ar/^{36}Ar	^{3}He/^{4}He (R/R$_A$)	^{3}He/^{4}He (R$_C$/R$_A$)	CO_2/^{3}He $\times10^{9}$
Colombia																			
Nev. del Ruiz	JCH-04	Fissure lavas	BA	Oliv	0.99	0.24	0.48	1.65	5.46	0.40	0.16	5.0	10.12 ± 0.03	0.0297 ± 0.0005	0.60	302.8 ± 0.1	7.96	8.46 ± 0.26	0.56
Galeras	GA1	Fissure lavas	BA	Oliv	1.07	1.19	0.22	1.25	4.09	0.39	0.62	54.6	9.83 ± 0.04	0.0284 ± 0.0007	3.08	304.9 ± 0.1	5.70	5.73 ± 0.12	0.66
	GA2	Fissure lavas	BA	Oliv	0.79	0.78	0.13	0.30	0.89	0.41	0.31	59.0	9.95 ± 0.08	0.0298 ± 0.0013	1.89	341.9 ± 0.3	6.87	6.90 ± 0.16	0.42
Ecuador																			
Cotopaxi	COT.LF.1B	Lava flow	A	Oliv	0.19	1.68	0.10	0.87	2.62	0.96	9.26	171.3	10.46 ± 0.18	-	1.75	332.2 ± 0.5	7.03	7.04 ± 0.28	5.64
				Opx	1.12	0.12	0.53	2.19	7.35	0.18	1.14	2.2	9.90 ± 0.02	0.0287 ± 0.0004	0.66	297.9 ± 0.1	2.00	2.22 ± 0.30	3.19
Reventador	REV.BB007 #16	Lava flow	A	Oliv	0.33	11.70	0.22	1.97	4.17	7.34	69.4	522.3	10.15 ± 0.08	0.0376 ± 0.0001	1.59	471.7 ± 0.1	6.97	6.98 ± 0.08	6.13
				Opx	0.44	3.23	1.50	6.67	21.90	1.84	8.63	21.5	9.97 ± 0.03	0.0306 ± 0.0001	1.75	303.9 ± 0.04	6.71	6.80 ± 0.13	2.83
Tungurahua	Tung 1100	Tephra deposits	A	Oliv	0.23	17.70	3.30	8.75	26.20	10.00	31.1	53.8	9.97 ± 0.02	0.0297 ± 0.0002	1.77	333.8 ± 0.2	7.05	7.08 ± 0.09	1.78
				Opx	0.89	2.55	2.88	5.88	19.60	0.87	0.70	8.9	9.98 ± 0.01	0.0294 ± 0.0002	2.92	300.0 ± 0.1	6.87	7.10 ± 0.12	0.28
	Tung 2006	Block PDC	A	Oliv	0.24	14.40	1.77	6.23	19.50	4.79	60.8	81.1	10.02 ± 0.02	0.0310 ± 0.0003	3.00	320.0 ± 0.2	7.37	7.40 ± 0.10	4.11
				Opx	0.87	1.40	1.35	4.33	14.30	0.97	0.84	10.4	9.97 ± 0.02	0.0293 ± 0.0002	1.45	302.3 ± 0.1	7.19	7.39 ± 0.11	0.58

Host rock chemical classification on the basis of SiO_2 contents: A (andesite), BA (basaltic-andesite)

Noble gas and CO_2 concentrations in mol g^{-1}

Mineral phases analyzed: Oliv (olivine), Opx (orthopyroxene)

Table 2

Noble gas compositions of fumarolic gases sampled at the central crater of Galeras, Colombia

Galeras	date	Lat, Long (N, W)	Temp. (^{o}C)	[He] ppm	CO_2 %	$^{40}Ar^*$ ppm	$^{4}He/^{20}Ne$	He/Ar^*	$^{40}Ar/^{36}Ar$	$^{3}He/^{4}He$ [a] (R/R_A)	$^{3}He/^{4}He$ [b] (R_C/R_A)	$CO_2/^{3}He$ $x10^{10}$
Central crater	14 Jul 2017	1.221, -75.360	91.3	2.18	93.41	-	7.29	-	-	8.01	8.33 ± 0.07	3.71
Central crater	14 Jul 2017	1.221, -75.359	87.5	1.93	96.15	1.40	29.63	1.38	302.1 ± 0.2	8.11	8.19 ± 0.07	4.38

[a] $R/R_A = {}^{3}He/{}^{4}He_{(meas.)}/{}^{3}He/{}^{4}He_{(air)}$ [$^{3}He/^{4}He_{(air)}=1.4\times10^{-6}$]

[b] R_C/R_A is the air corrected He isotopic ratio based on the $^{4}He/^{20}Ne$ ratio (Giggenbach et al., 1993).

Note: only $^{40}Ar/^{36}Ar > 300$ are reported in order to avoid overestimation of $^{40}Ar^*$

Table 3

Helium isotope data compilation for Northern Volcanic Zone Quaternary volcanoes and hydrothermal areas.

		Low-T hydrothermal sources $^3He/^4He$ (R_C/R_A)				High-T fumarolic gases $^3He/^4He$ (R_C/R_A)				Fluid Inclusions (Oliv, Opx) $^3He/^4He$ (R_C/R_A)			
Colombia	Latitude	*Max*	Avg.	Nr. samples	Ref.	*Max*	Avg.	Nr. samples	Ref.	*Max*	Avg.	Nr. samples	Ref.
Nevado del Ruiz	4.89	6.4	3.9±1.4	22	1,2	6.3	---	1	1	8.5	---	1	*
Cerro Machín	4.48	5.9	5.2±0.9	2	3	6.75	---	1	4	---	---	n/d	---
Purace	2.31	6.7	4.9±1.3	8	5	7.1	6.4±0.5	4	5,6	---	---	n/d	---
Galeras	1.22	4.6	2.0±1.3	7	7	8.8	7.7±0.9	20	4, 7, *	6.9	6.3±0.8	2	*
Cumbal	0.94	5.5	---	1	8	7.9	6.3±0.9	10	4, 8	---	---	n/d	---
Ecuador													
Reventador	-0.08	---	---	n/d	---	---	---	n/d	---	7.0	6.9±0.1	2	*
Guagua Pichincha	-0.17	3.4	---	1	9	4.1	4.1±0.2	2	p.c.	---	---	---	---
Cotopaxi	-0.70	6.8	---	1	9	---	---	---	---	7.0	4.6±3.4	2	*
Tungurahua	-1.45	2.7	4.6±0.7	2	9	---	---	---	---	7.4	7.2±0.2	4	*
Chimborazo	-1.47	2.1	---	1	9	---	---	---	---	---	---	---	---
Other sites													
Cuicocha	0.29	6.3	---	1	9								
Pululahua	0.01	3.7	---	1	9								
El Pisque Balneario	0.00	4.2	---	1	9								
Balneario Oyacachi	-0.22	2.6	---	1	9								
Jamanco	-0.38	7.1	---	1	9								
Cachiyacu Cueva	-0.41	6.5	---	1	9								
Cachiyacu	-0.41	4.2	---	1	9								
Aguas calientes	-0.44	3.4	---	1	9								
Quilotoa	-0.86	2.1	---	1	9								
S. Vicente	-2.23	0.1	---	1	9								
Jesus Maria	-2.63	0.3	---	1	9								
Guapan	-2.71	0.7	---	1	9								
El Mozo	-3.44	0.2	---	1	9								
Portovelo	-3.70	0.9	---	1	9								

Max: maximum R_C/R_A value for a given sampling media

Avg: *average of all samples for a given sampling media ± 1 σ*

Ref. 1. Williams et al., 1987; **2.** Sano et al., 1990; **3.** Inguaggiato et al., 2016; **4.** Sano and Williams, 1996; **5.** Sturchio et al., 1993; **6.** Maldonado et al., 2017; **7.** Sano et al., 1997; **8.** Lewicki et al., 2000; **9.** Inguaggiato et al., 2010. *This investigation; **p.c.** personal communication (unpublished)

1258